

A recipe for exotic continental fragment formation: automated data analysis of rift models

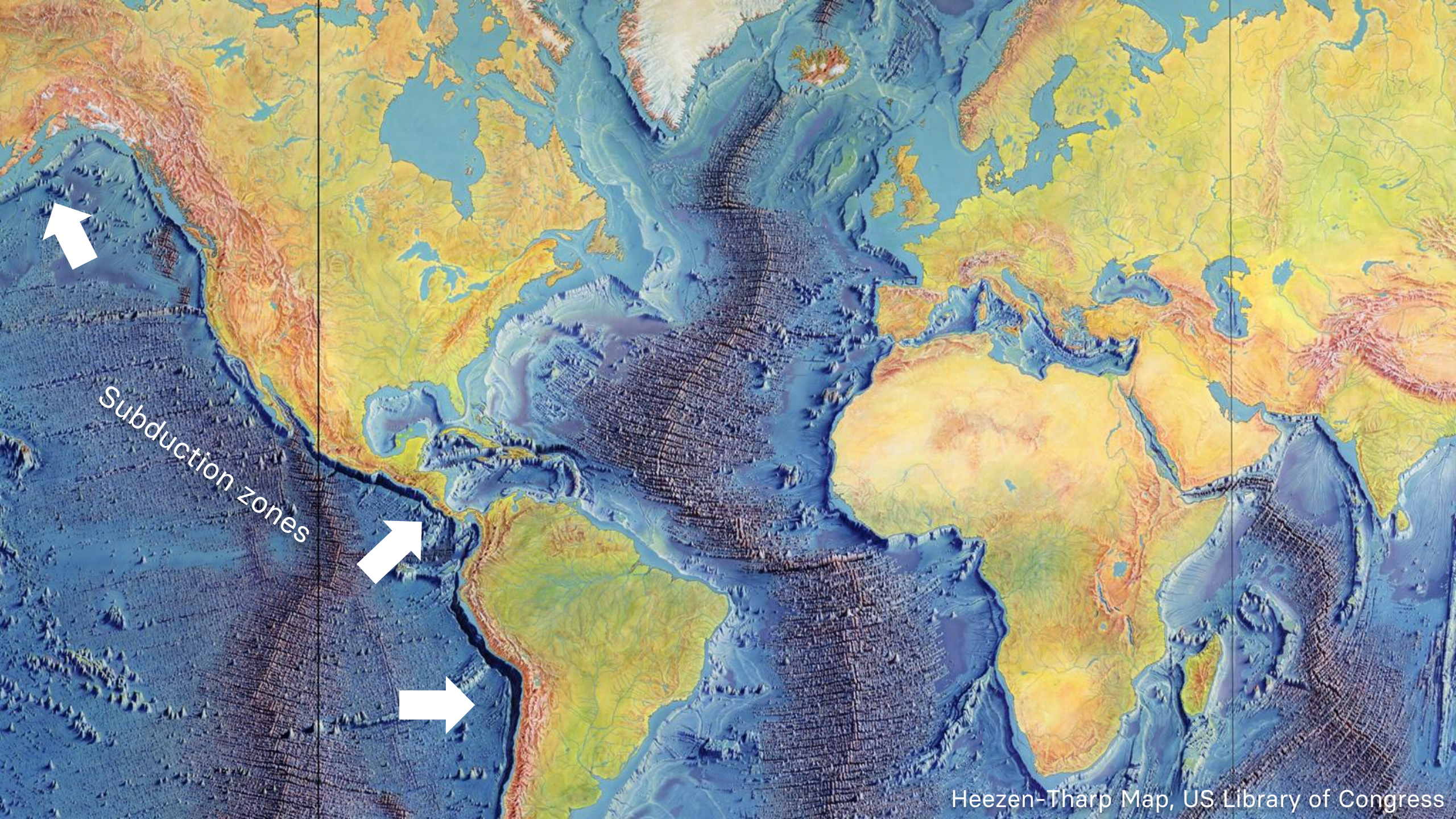
Alan Yu, Erkan Gun, Ken McCaffrey, Phil Heron



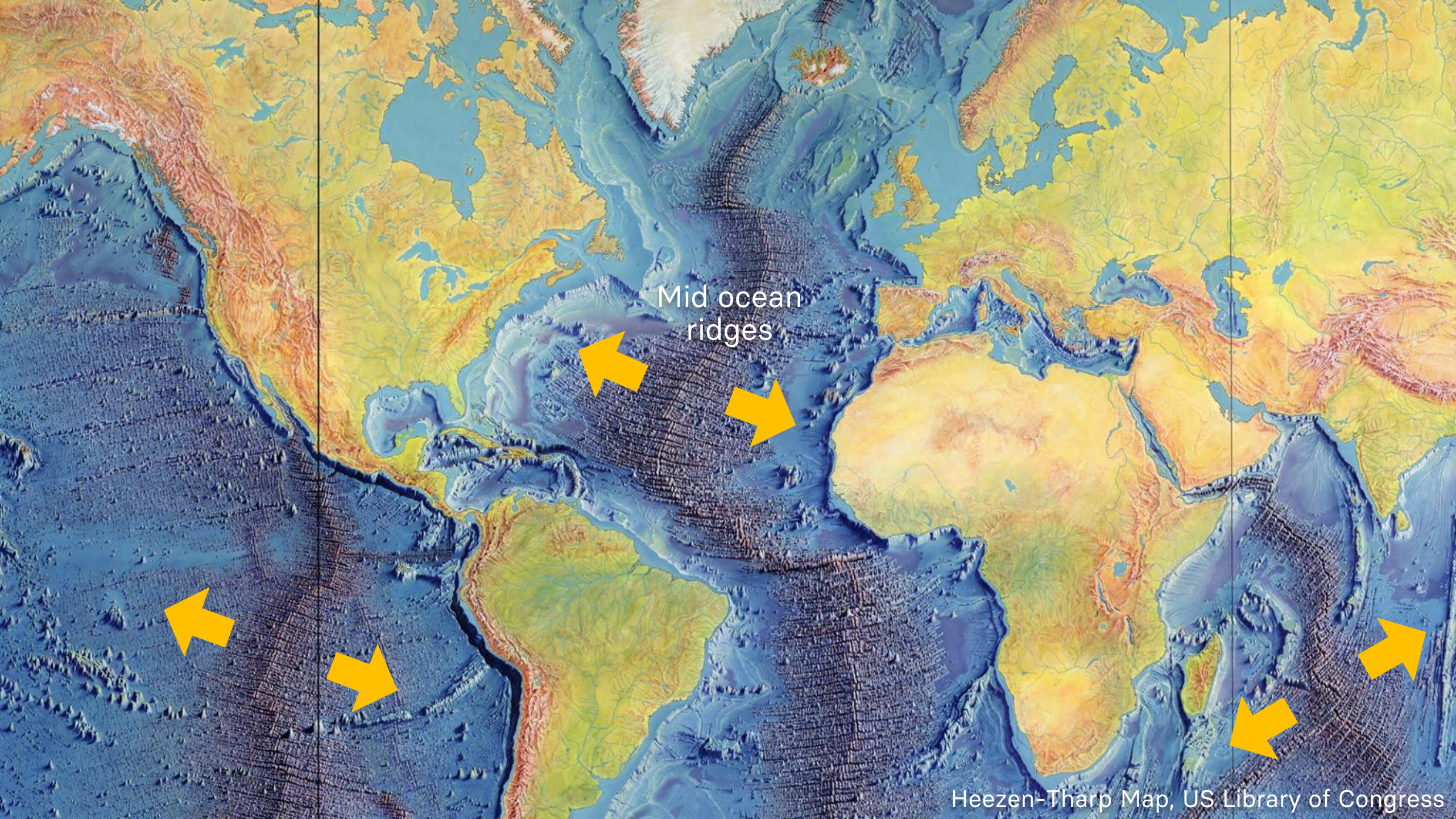
Heezen-Tharp Map, US Library of Congress



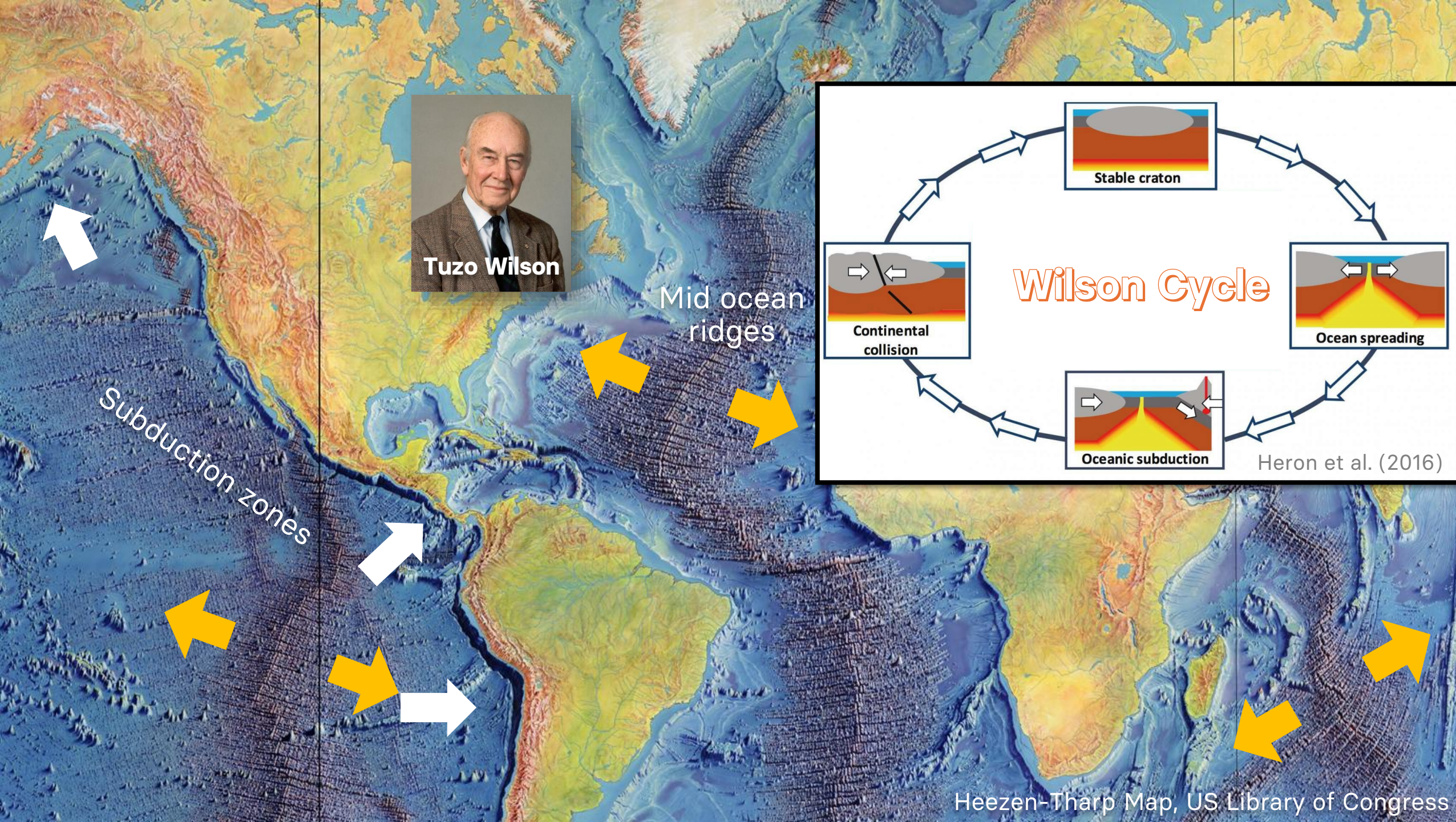
Heezen-Tharp Map, US Library of Congress



Heezen-Tharp Map, US Library of Congress

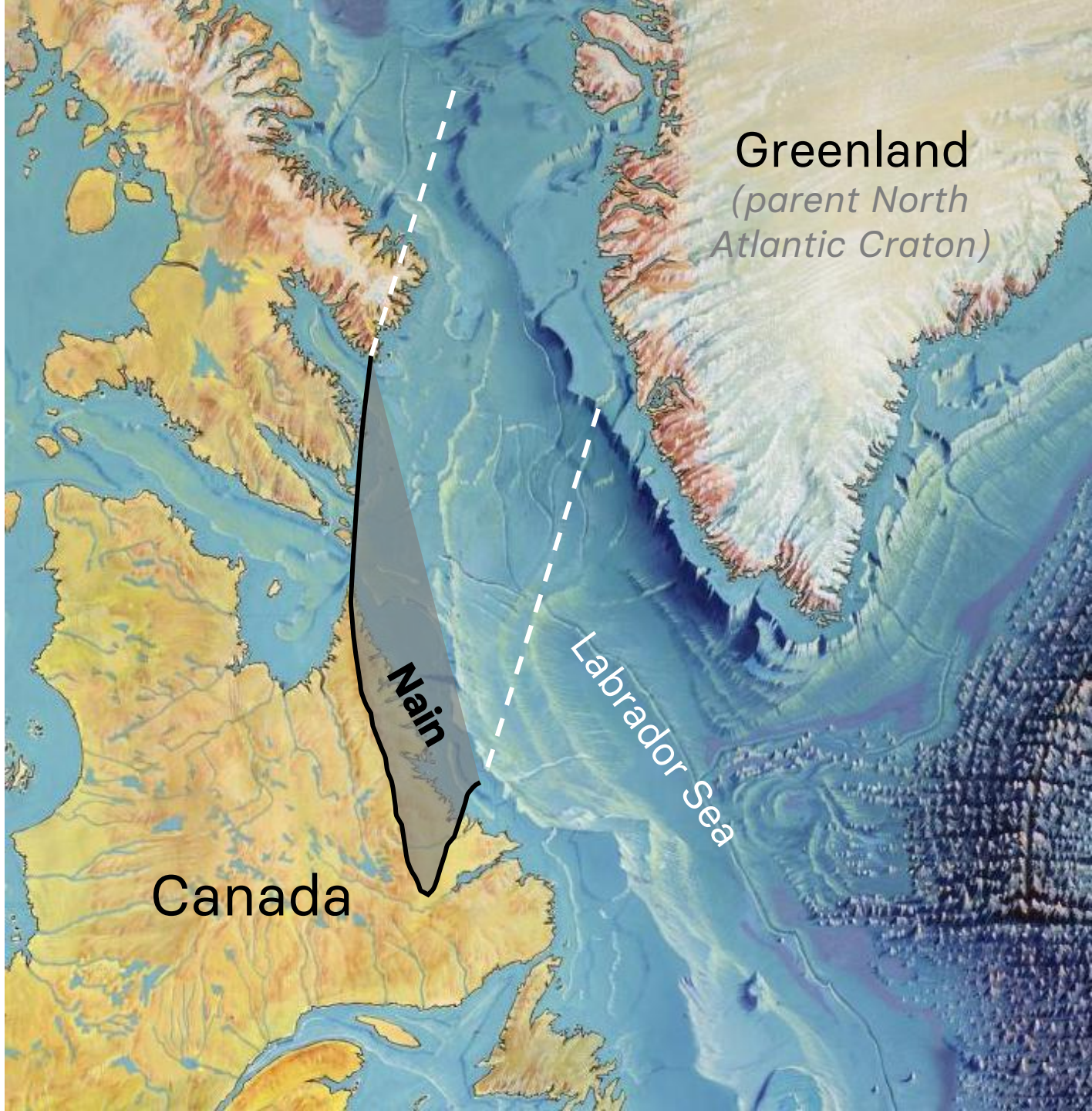


Heezen-Tharp Map, US Library of Congress



Continental fragment

- The general view of Wilson Cycle does not explain more **nuanced** tectonic scenarios.
- The opening of the Labrador Sea left a piece of Greenland (the **Nain Province**) in Eastern Canada.
- Continental fragment is **a small piece of continent** separated from its parent plate.
- They share the **same geological history** prior to separation.



Continental fragment

North Atlantic Ocean

Nain Province

Lewisian Complex

South Atlantic Ocean

São Luís Craton

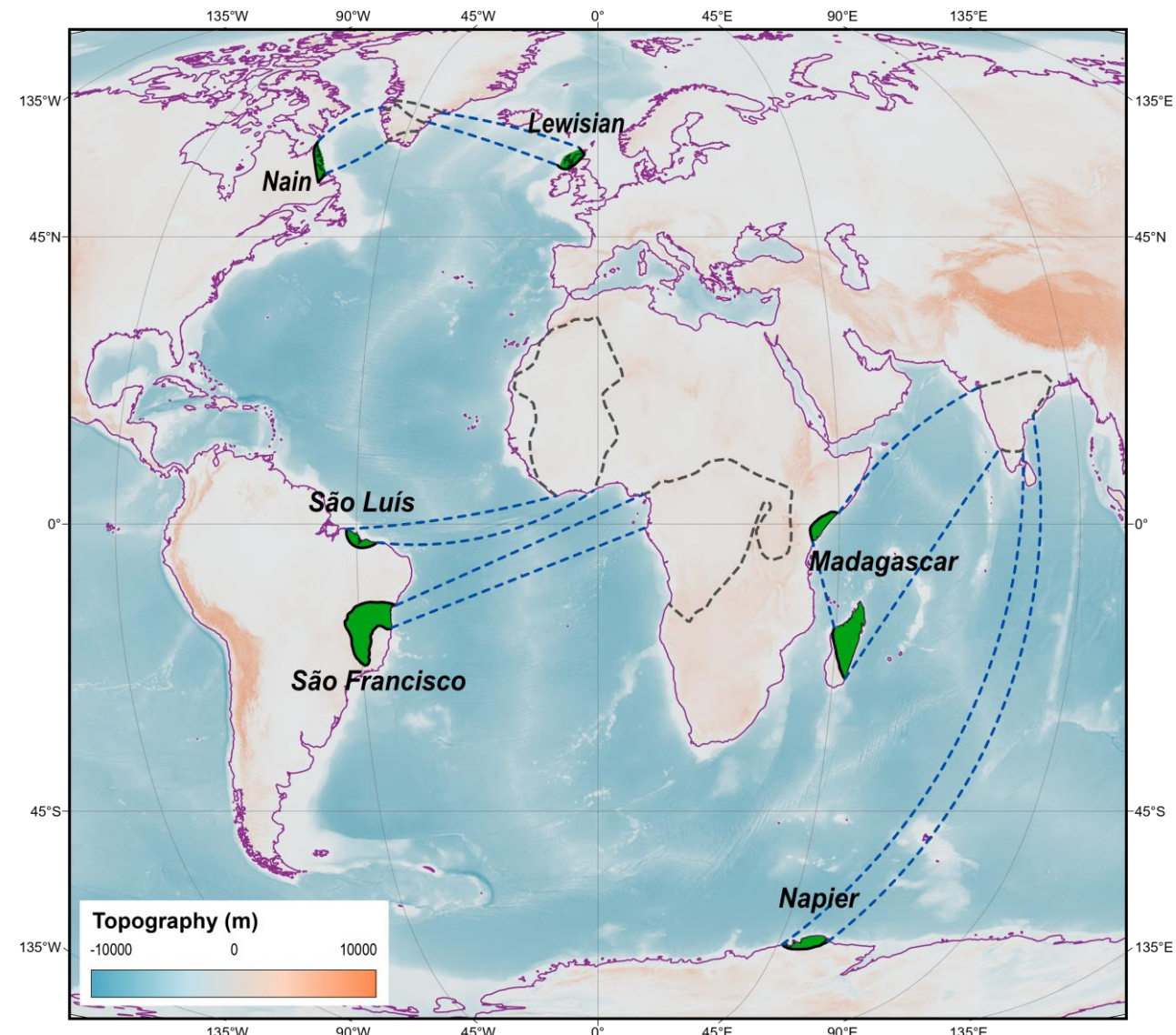
São Francisco Craton

Indian Ocean

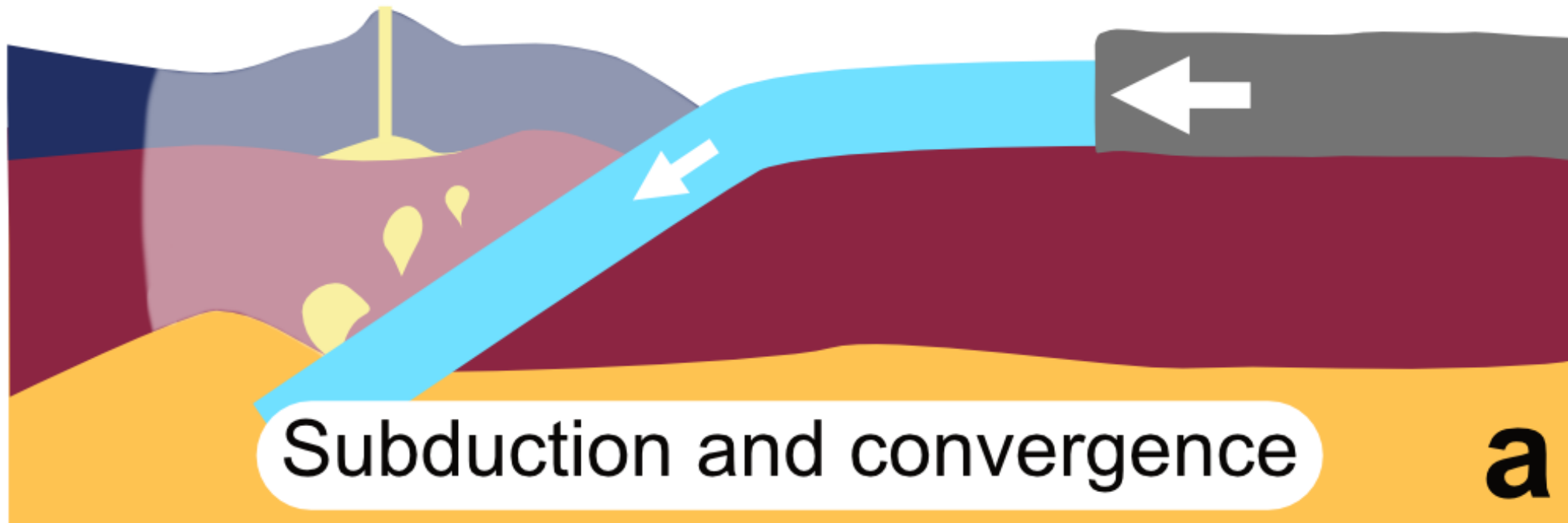
Madagascar

Napier Complex

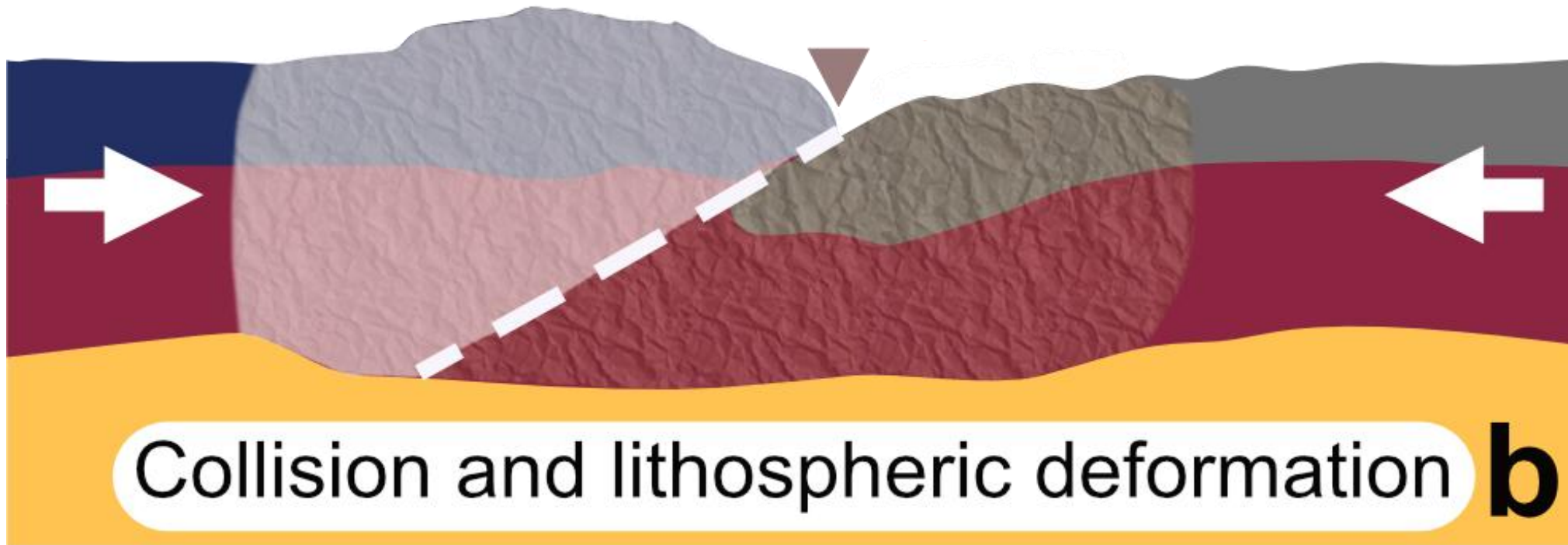
How did they form?



Wilson Cycle



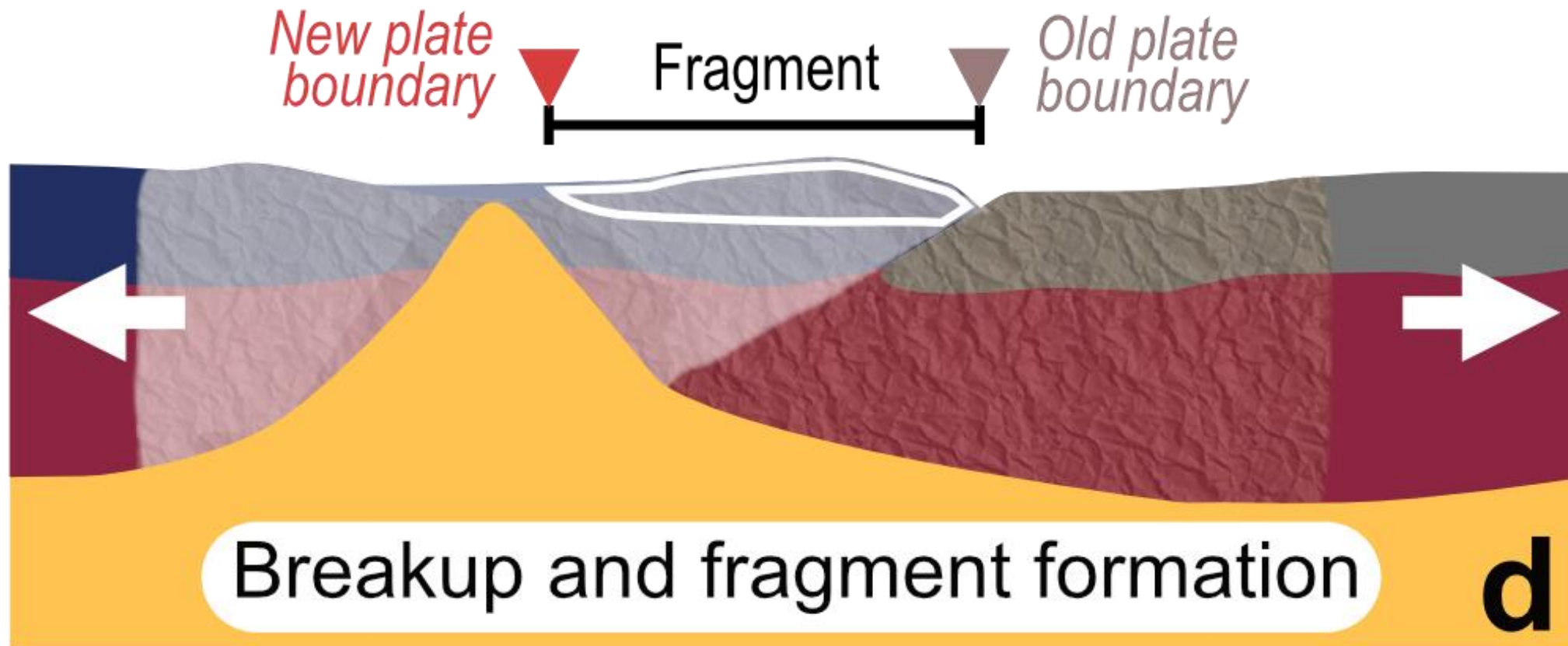
Wilson Cycle



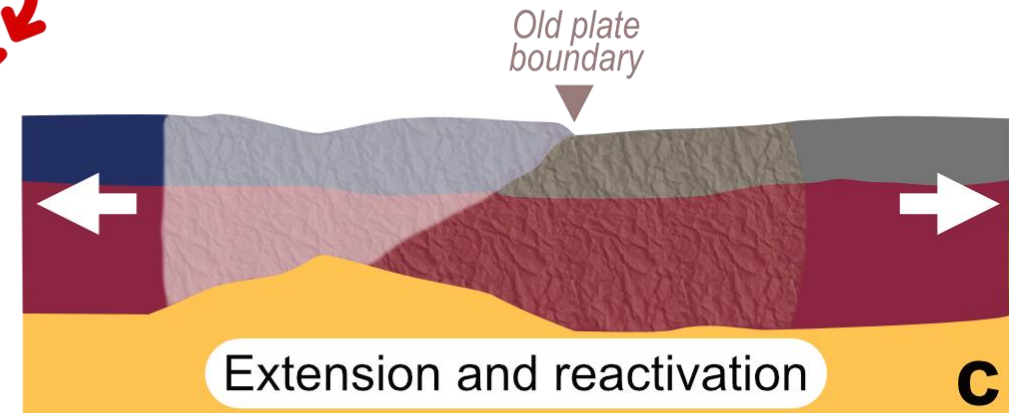
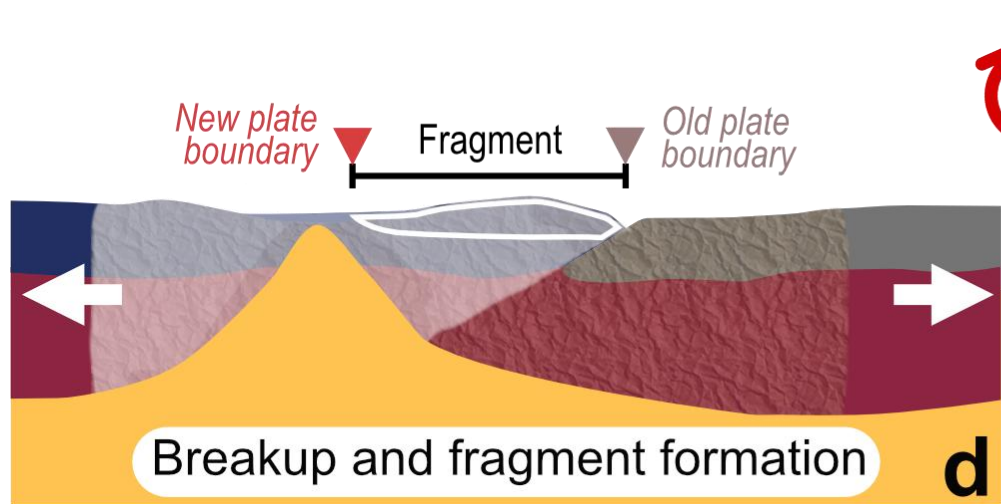
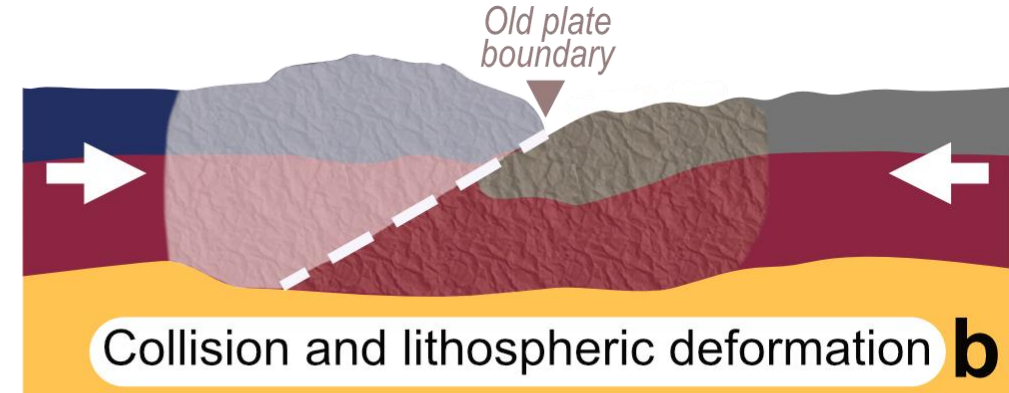
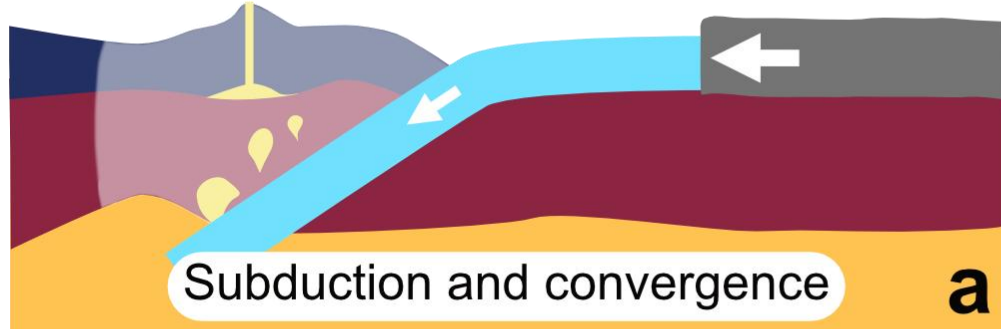
Wilson Cycle



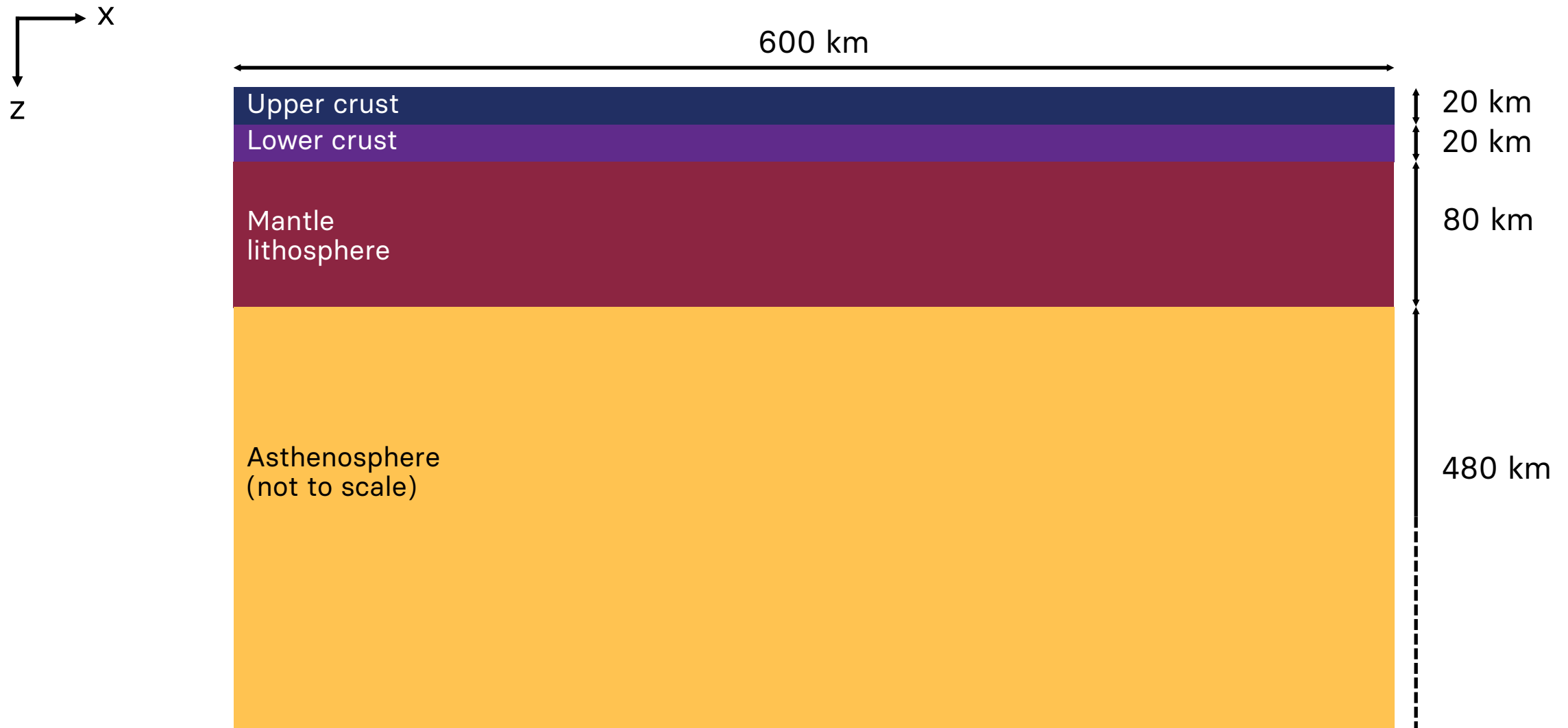
Wilson Cycle



Wilson Cycle



Model setup



Model setup

X
Z

600 km



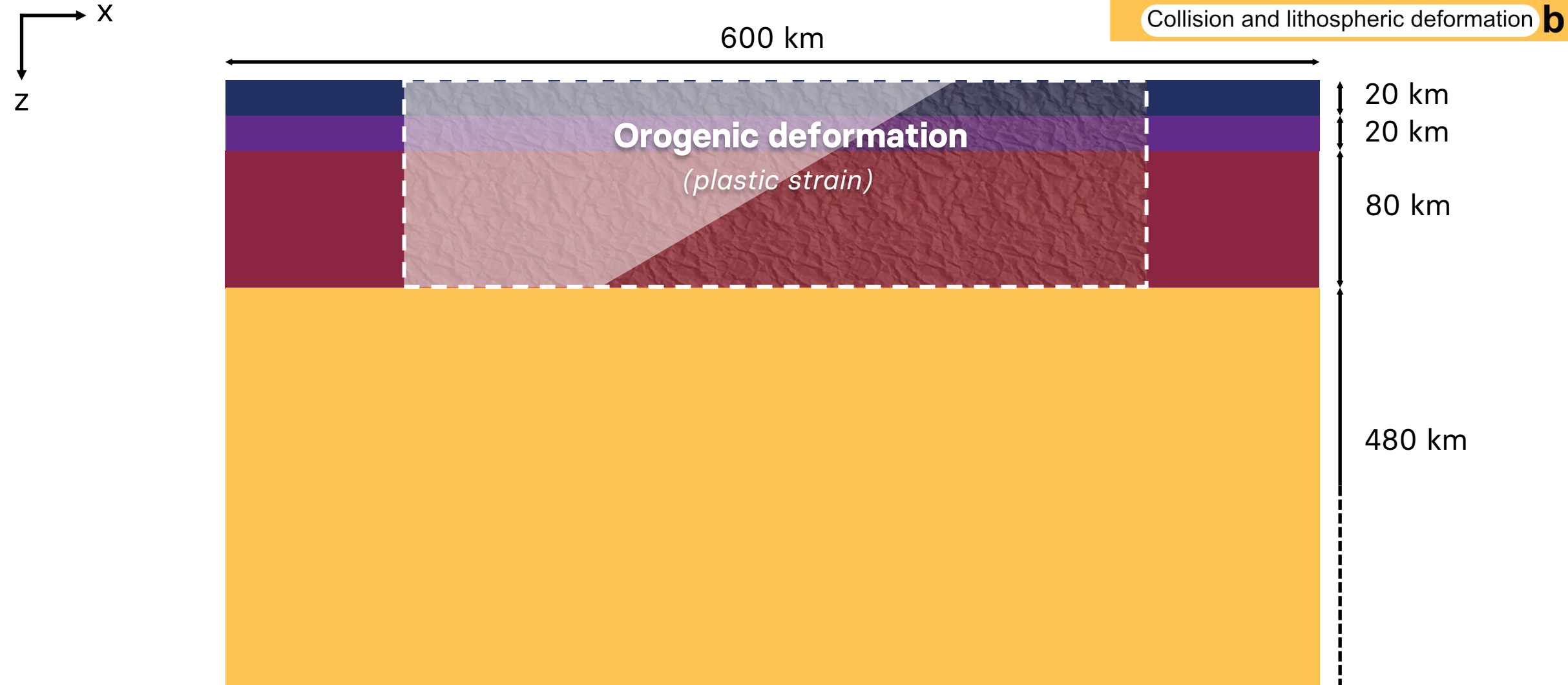
20 km
20 km
80 km
480 km

Subduction and convergence

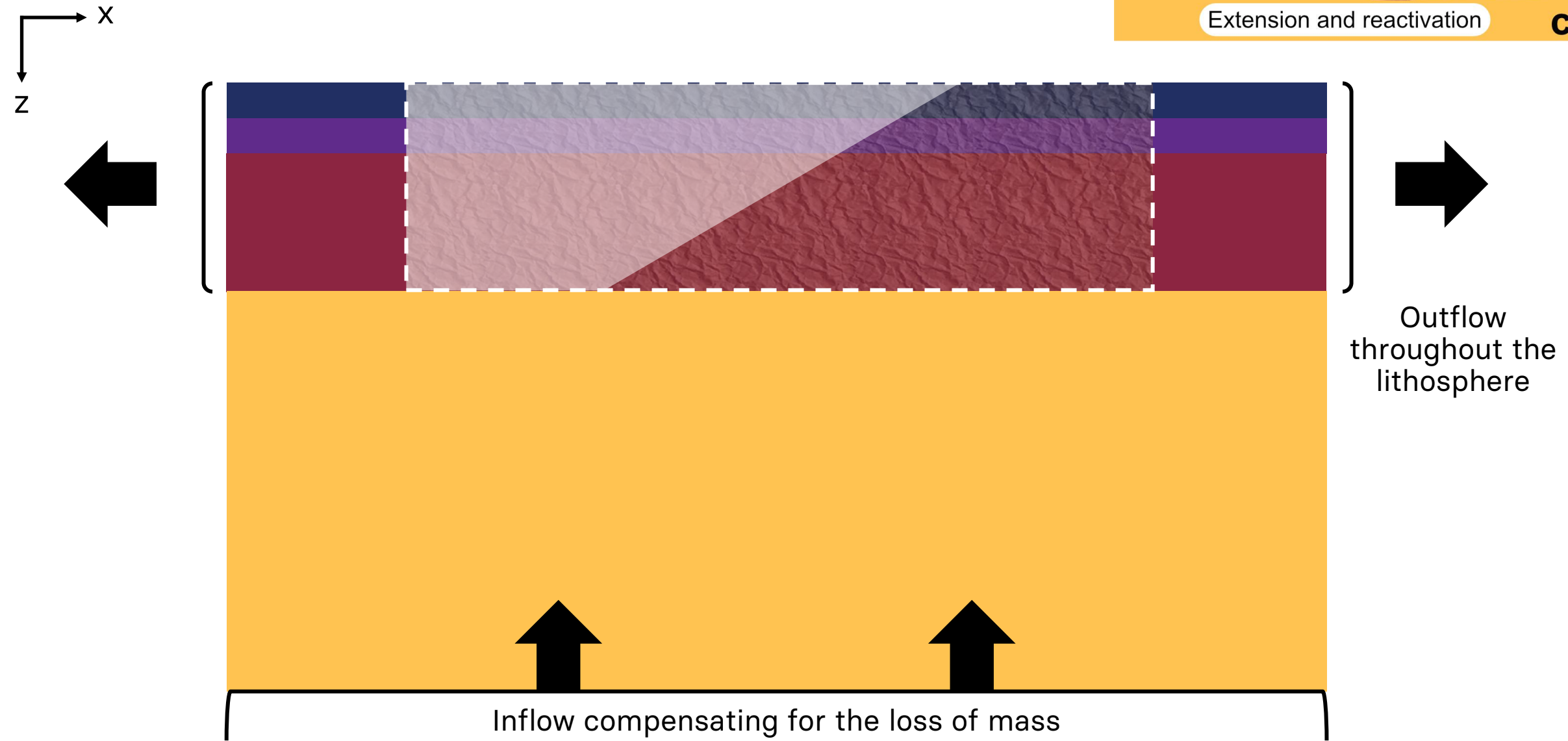
a

$$f = \frac{\eta_{\text{Upper plate margin}}}{\eta_{\text{Lower plate margin}}}$$

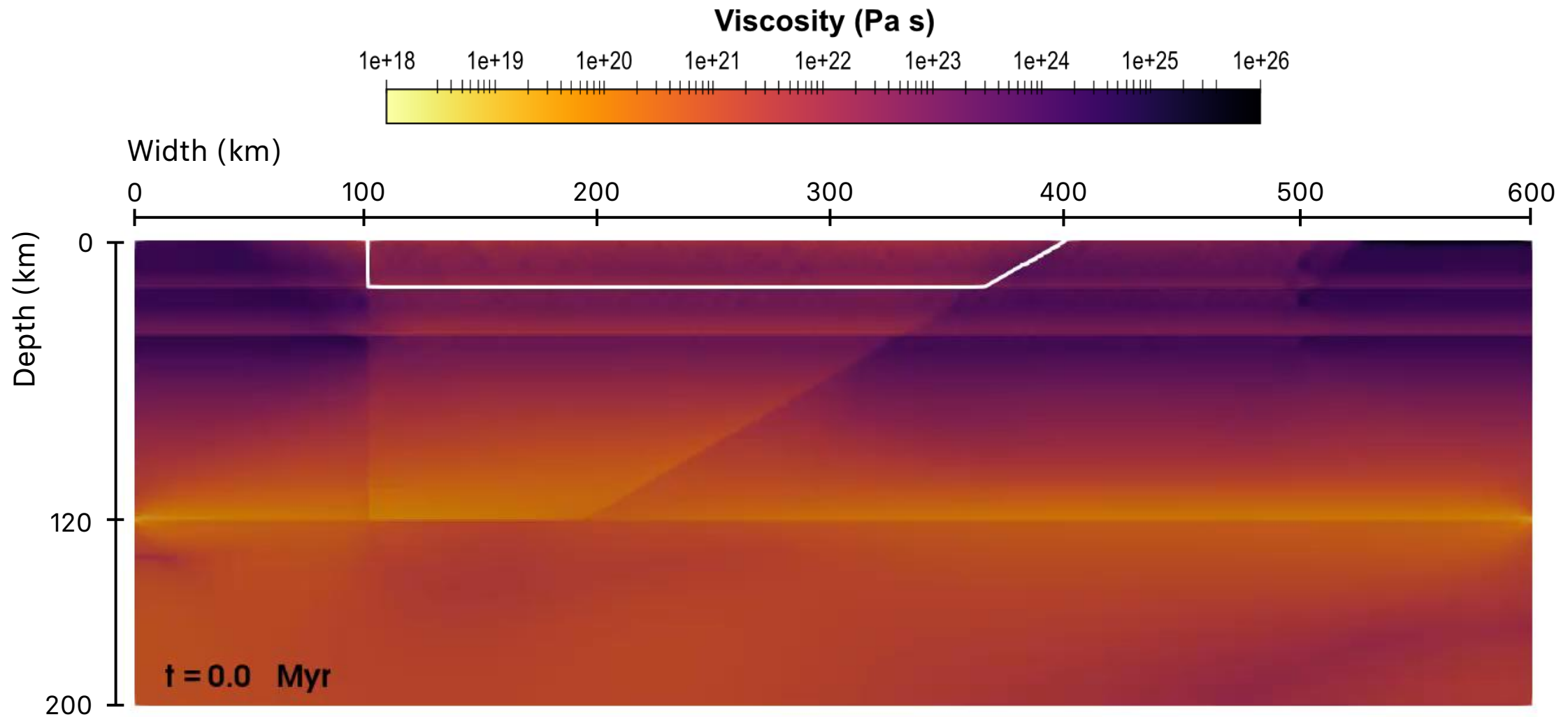
Model setup



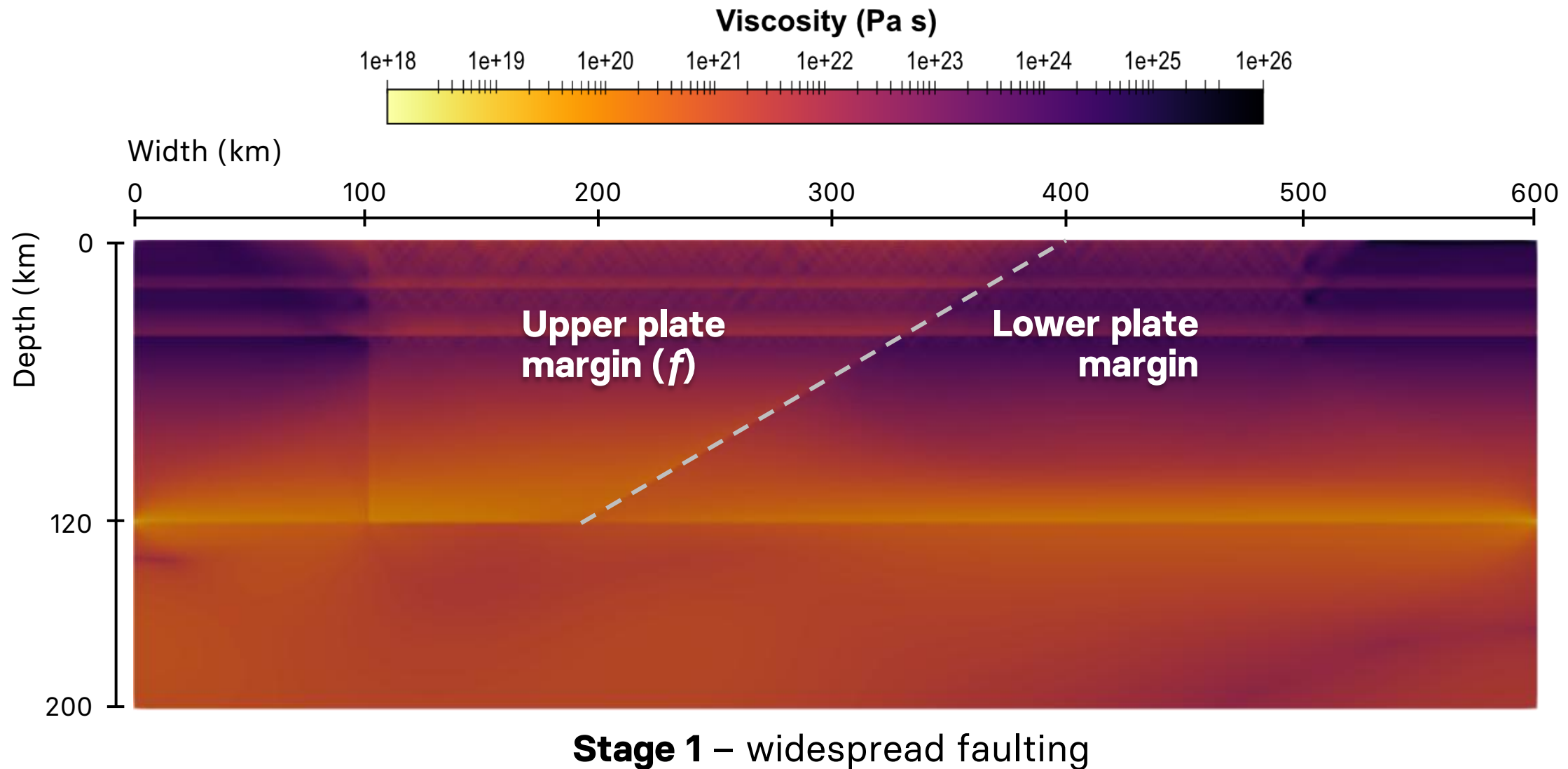
Model setup



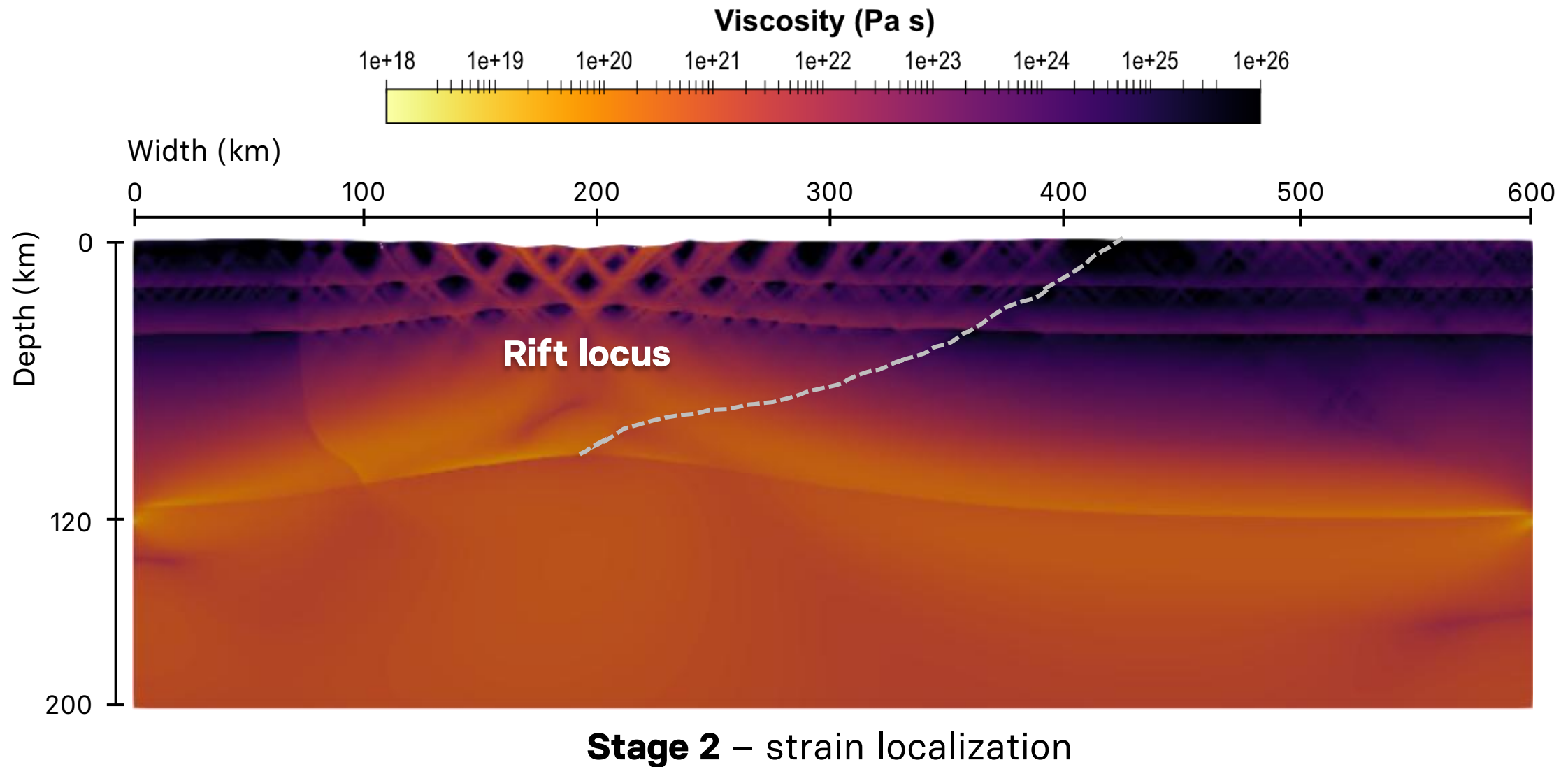
Reference model



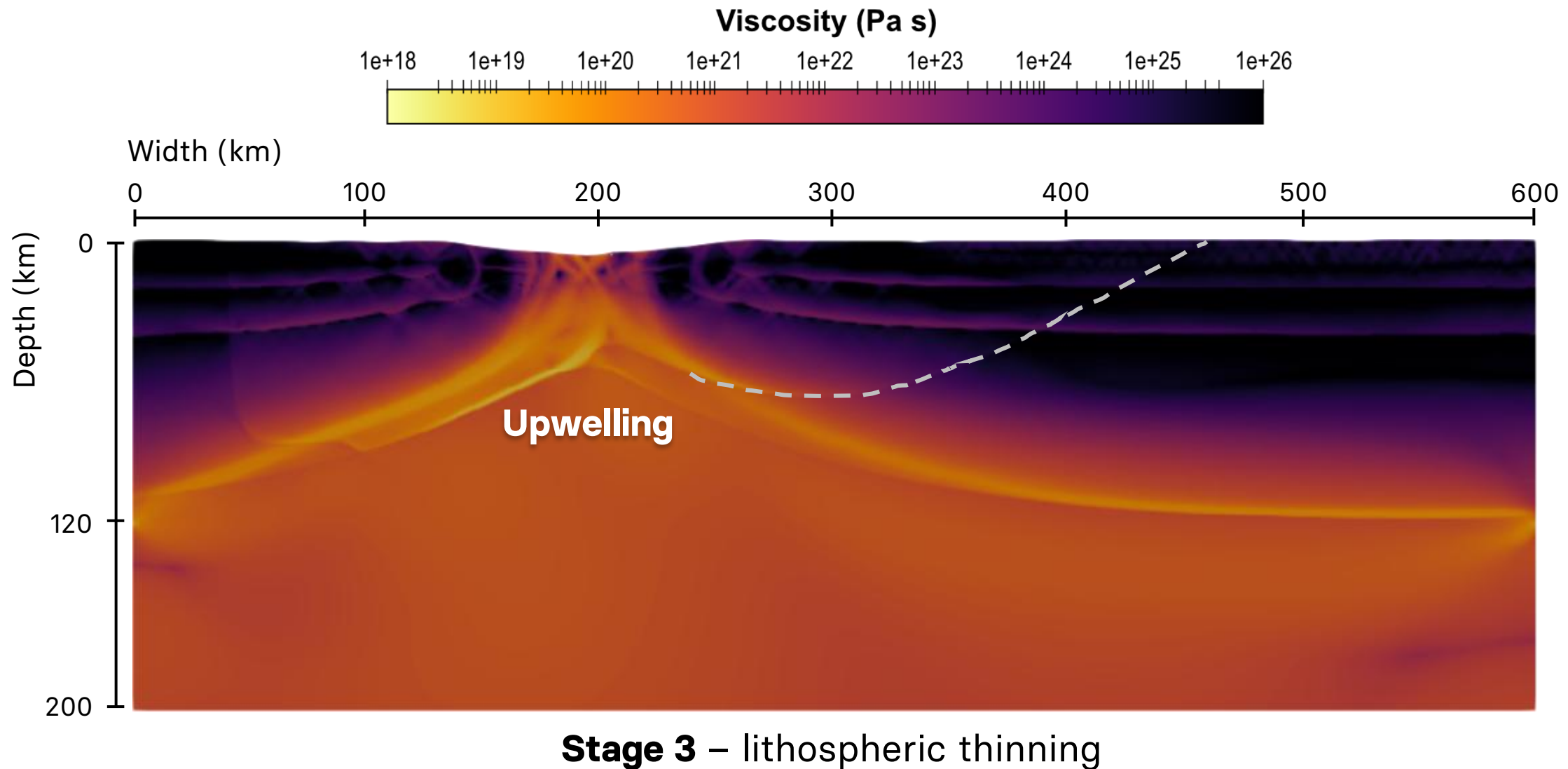
Reference model



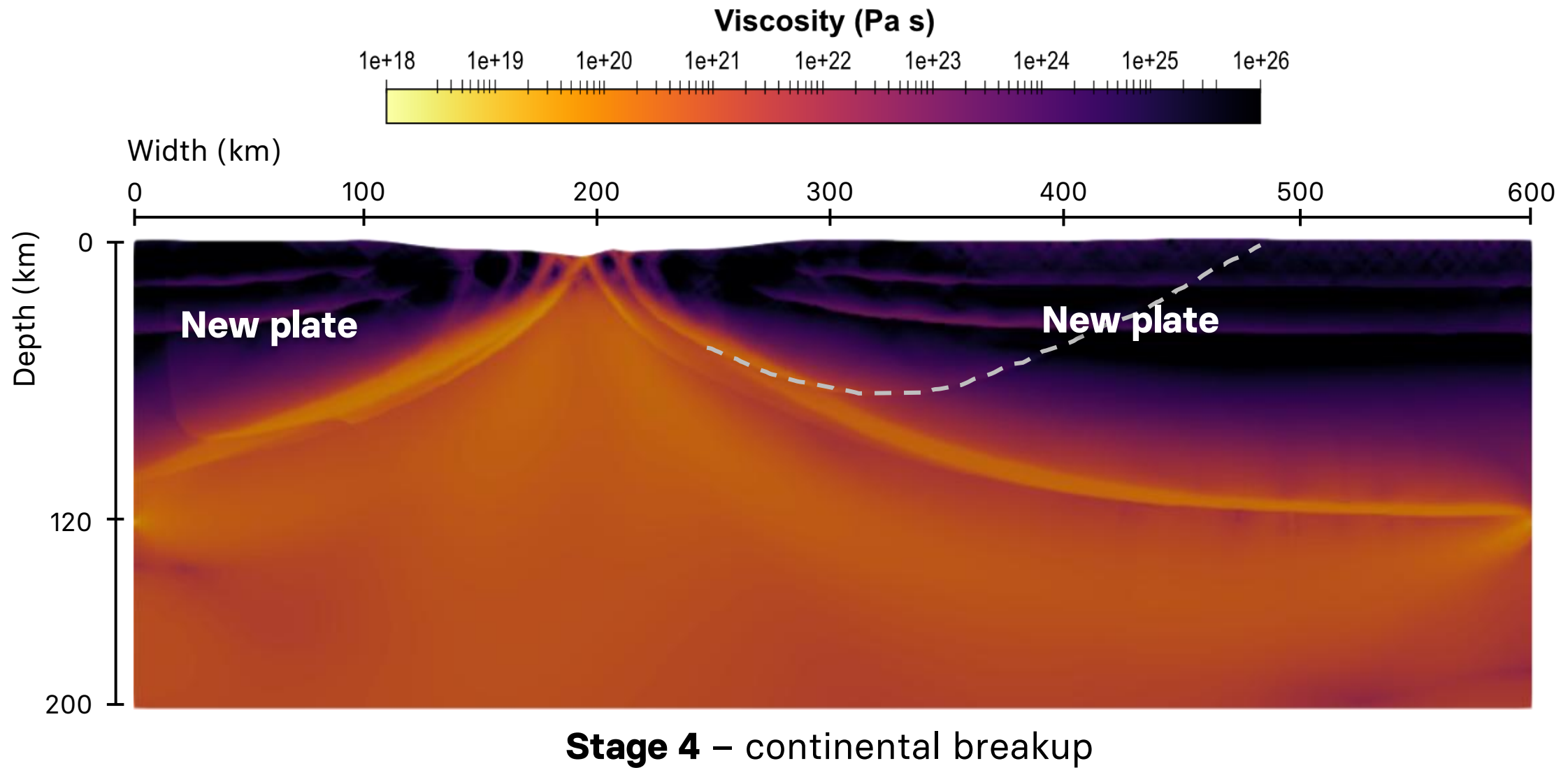
Reference model



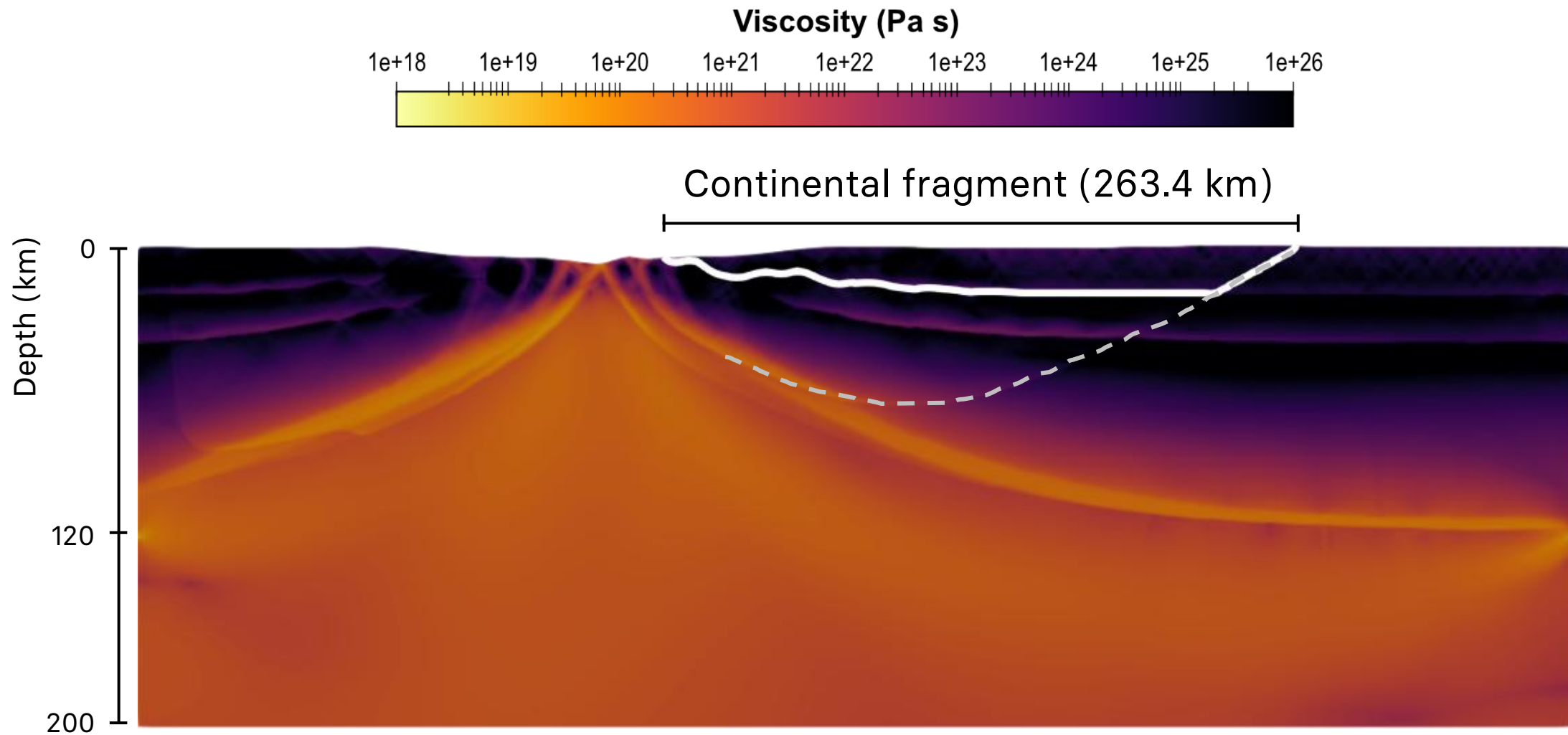
Reference model



Reference model



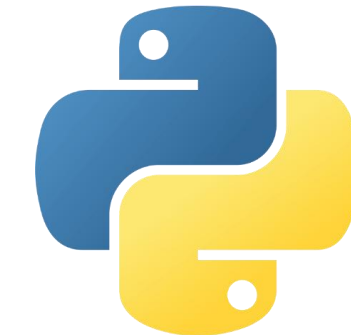
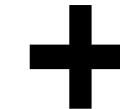
Reference model



Automated data analysis

- From the reference model, we systematically tested **8 physical parameters**, resulting in **94 models** and over **5000 output files**.
- We implemented an **automated system** that sorts through and analyzes all output files.
- This system detects **the time of continental breakup** (i.e., when asthenospheric rocks ascends to the surface) and measures **the width of the continental fragment** (the width of upper crust of the separated continent).

ParaView



Python

Automated data analysis

Model output

solution-00000.0000.vtu

solution-00000.pvtu

solution-00001.0000.vtu

solution-00001.pvtu

solution-00002.0000.vtu

solution-00002.pytut

solution-00002_0000.vtu

solution-00003.pytui

solution-00003 0000.vtu

solution_00004.pytut

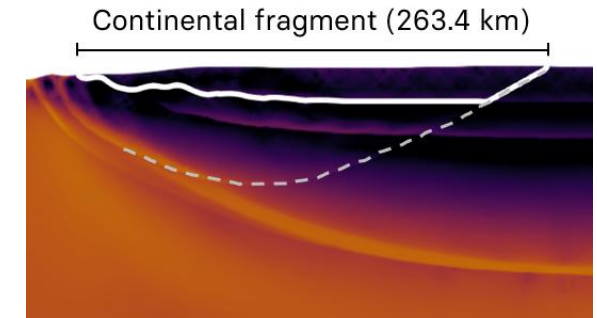
solution_00004_00004.htm

3

0.00E+03	8.00E-03	0.00E+00	1.10E-08	-2.88E-09	0	10	971	1.00E+00	3.00E+00	2.88E+00	1.00E+00
1.00E+03	8.00E-03	0.00E+00	2.88E-09	-7.20E-10	0	41	1032	1.00E+00	3.00E+00	2.88E+00	1.00E+00
2.00E+03	8.00E-03	0.00E+00	5.76E-09	-1.80E-10	0	72	1064	1.00E+00	3.00E+00	2.88E+00	1.00E+00
3.00E+03	8.00E-03	0.00E+00	9.21E-09	-2.88E-10	0	103	1094	1.00E+00	3.00E+00	2.88E+00	1.00E+00
4.00E+03	8.00E-03	0.00E+00	1.29E-08	-4.05E-10	0	134	1066	1.00E+00	3.00E+00	2.88E+00	1.00E+00
5.00E+03	8.00E-03	0.00E+00	1.66E-08	-5.22E-10	0	165	1137	1.00E+00	3.00E+00	2.88E+00	1.00E+00
6.00E+03	8.00E-03	0.00E+00	2.03E-08	-6.40E-10	0	196	1157	1.00E+00	3.00E+00	2.88E+00	1.00E+00
7.00E+03	8.00E-03	0.00E+00	2.40E-08	-7.58E-10	0	227	1188	1.00E+00	3.00E+00	2.88E+00	1.00E+00
8.00E+03	8.00E-03	0.00E+00	2.77E-08	-8.75E-10	0	258	1208	1.00E+00	3.00E+00	2.88E+00	1.00E+00
9.00E+03	8.00E-03	0.00E+00	3.14E-08	-9.93E-10	0	289	1228	1.00E+00	3.00E+00	2.88E+00	1.00E+00
1.00E+04	8.00E-03	0.00E+00	3.51E-08	-1.11E-09	0	320	1248	1.00E+00	3.00E+00	2.88E+00	1.00E+00
1.10E+04	8.00E-03	0.00E+00	3.88E-08	-1.23E-09	0	351	1268	1.00E+00	3.00E+00	2.88E+00	1.00E+00
1.20E+04	8.00E-03	0.00E+00	4.25E-08	-1.35E-09	0	382	1288	1.00E+00	3.00E+00	2.88E+00	1.00E+00
1.30E+04	8.00E-03	0.00E+00	4.62E-08	-1.47E-09	0	413	1308	1.00E+00	3.00E+00	2.88E+00	1.00E+00
1.40E+04	8.00E-03	0.00E+00	5.00E-08	-1.59E-09	0	444	1328	1.00E+00	3.00E+00	2.88E+00	1.00E+00
1.50E+04	8.00E-03	0.00E+00	5.37E-08	-1.71E-09	0	475	1348	1.00E+00	3.00E+00	2.88E+00	1.00E+00
1.60E+04	8.00E-03	0.00E+00	5.74E-08	-1.83E-09	0	506	1368	1.00E+00	3.00E+00	2.88E+00	1.00E+00
1.70E+04	8.00E-03	0.00E+00	6.11E-08	-1.95E-09	0	537	1388	1.00E+00	3.00E+00	2.88E+00	1.00E+00
1.80E+04	8.00E-03	0.00E+00	6.48E-08	-2.07E-09	0	568	1408	1.00E+00	3.00E+00	2.88E+00	1.00E+00
1.90E+04	8.00E-03	0.00E+00	6.85E-08	-2.19E-09	0	599	1428	1.00E+00	3.00E+00	2.88E+00	1.00E+00
2.00E+04	8.00E-03	0.00E+00	7.22E-08	-2.31E-09	0	630	1448	1.00E+00	3.00E+00	2.88E+00	1.00E+00
2.10E+04	8.00E-03	0.00E+00	7.59E-08	-2.43E-09	0	661	1468	1.00E+00	3.00E+00	2.88E+00	1.00E+00
2.20E+04	8.00E-03	0.00E+00	7.96E-08	-2.55E-09	0	692	1488	1.00E+00	3.00E+00	2.88E+00	1.00E+00
2.30E+04	8.00E-03	0.00E+00	8.33E-08	-2.67E-09	0	733	1508	1.00E+00	3.00E+00	2.88E+00	1.00E+00
2.40E+04	8.00E-03	0.00E+00	8.70E-08	-2.79E-09	0	754	1528	1.00E+00	3.00E+00	2.88E+00	1.00E+00
2.50E+04	8.00E-03	0.00E+00	9.07E-08	-2.91E-09	0	785	1548	1.00E+00	3.00E+00	2.88E+00	1.00E+00
2.60E+04	8.00E-03	0.00E+00	9.44E-08	-3.03E-09	0	816	1568	1.00E+00	3.00E+00	2.88E+00	1.00E+00
2.70E+04	8.00E-03	0.00E+00	9.81E-08	-3.15E-09	0	847	1588	1.00E+00	3.00E+00	2.88E+00	1.00E+00
2.80E+04	8.00E-03	0.00E+00	1.018E-07	-3.27E-09	0	878	1608	1.00E+00	3.00E+00	2.88E+00	1.00E+00
2.90E+04	8.00E-03	0.00E+00	1.055E-07	-3.39E-09	0	909	1628	1.00E+00	3.00E+00	2.88E+00	1.00E+00
3.00E+04	8.00E-03	0.00E+00	1.092E-07	-3.51E-09	0	940	1648	1.00E+00	3.00E+00	2.88E+00	1.00E+00
3.10E+04	8.00E-03	0.00E+00	1.129E-07	-3.63E-09	0	971	1668	1.00E+00	3.00E+00	2.88E+00	1.00E+00
3.20E+04	8.00E-03	0.00E+00	1.166E-07	-3.75E-09	0	1002	1688	1.00E+00	3.00E+00	2.88E+00	1.00E+00
3.30E+04	8.00E-03	0.00E+00	1.203E-07	-3.87E-09	0	1033	1708	1.00E+00	3.00E+00	2.88E+00	1.00E+00
3.40E+04	8.00E-03	0.00E+00	1.240E-07	-3.99E-09	0	1064	1728	1.00E+00	3.00E+00	2.88E+00	1.00E+00
3.50E+04	8.00E-03	0.00E+00	1.277E-07	-4.11E-09	0	1095	1748	1.00E+00	3.00E+00	2.88E+00	1.00E+00
3.60E+04	8.00E-03	0.00E+00	1.314E-07	-4.23E-09	0	1126	1768	1.00E+00	3.00E+00	2.88E+00	1.00E+00
3.70E+04	8.00E-03	0.00E+00	1.351E-07	-4.35E-09	0	1157	1788	1.00E+00	3.00E+00	2.88E+00	1.00E+00
3.80E+04	8.00E-03	0.00E+00	1.388E-07	-4.47E-09	0	1188	1808	1.00E+00	3.00E+00	2.88E+00	1.00E+00
3.90E+04	8.00E-03	0.00E+00	1.425E-07	-4.59E-09	0	1219	1828	1.00E+00	3.00E+00	2.88E+00	1.00E+00
4.00E+04	8.00E-03	0.00E+00	1.462E-07	-4.71E-09	0	1250	1848	1.00E+00	3.00E+00	2.88E+00	1.00E+00
4.10E+04	8.00E-03	0.00E+00	1.499E-07	-4.83E-09	0	1281	1868	1.00E+00	3.00E+00	2.88E+00	1.00E+00
4.20E+04	8.00E-03	0.00E+00	1.536E-07	-4.95E-09	0	1312	1888	1.00E+00	3.00E+00	2.88E+00	1.00E+00
4.30E+04	8.00E-03	0.00E+00	1.573E-07	-5.07E-09	0	1343	1908	1.00E+00	3.00E+00	2.88E+00	1.00E+00
4.40E+04	8.00E-03	0.00E+00	1.610E-07	-5.19E-09	0	1374	1928	1.00E+00	3.00E+00	2.88E+00	1.00E+00
4.50E+04	8.00E-03	0.00E+00	1.647E-07	-5.31E-09	0	1405	1948	1.00E+00	3.00E+00	2.88E+00	1.00E+00
4.60E+04	8.00E-03	0.00E+00	1.684E-07	-5.43E-09	0	1436	1968	1.00E+00	3.00E+00	2.88E+00	1.00E+00
4.70E+04	8.00E-03	0.00E+00	1.721E-07	-5.55E-09	0	1467	1988	1.00E+00	3.00E+00	2.88E+00	1.00E+00
4.80E+04	8.00E-03	0.00E+00	1.758E-07	-5.67E-09	0	1508	2008	1.00E+00	3.00E+00	2.88E+00	1.00E+00
4.90E+04	8.00E-03	0.00E+00	1.795E-07	-5.79E-09	0	1539	2028	1.00E+00	3.00E+00	2.88E+00	1.00E+00
5.00E+04	8.00E-03	0.00E+00	1.832E-07	-5.91E-09	0	1570	2048	1.00E+00	3.00E+00	2.88E+00	1.00E+00
5.10E+04	8.00E-03	0.00E+00	1.869E-07	-6.03E-09	0	1601	2068	1.00E+00	3.00E+00	2.88E+00	1.00E+00
5.20E+04	8.00E-03	0.00E+00	1.906E-07	-6.15E-09	0	1632	2088	1.00E+00	3.00E+00	2.88E+00	1.00E+00
5.30E+04	8.00E-03	0.00E+00	1.943E-07	-6.27E-09	0	1663	2108	1.00E+00	3.00E+00	2.88E+00	1.00E+00
5.40E+04	8.00E-03	0.00E+00	1.980E-07	-6.39E-09	0	1694	2128	1.00E+00	3.00E+00	2.88E+00	1.00E+00
5.50E+04	8.00E-03	0.00E+00	2.017E-07	-6.51E-09	0	1725	2148	1.00E+00	3.00E+00	2.88E+00	1.00E+00
5.60E+04	8.00E-03	0.00E+00	2.054E-07	-6.63E-09	0	1756	2168	1.00E+00	3.00E+00	2.88E+00	1.00E+00
5.70E+04	8.00E-03	0.00E+00	2.091E-07	-6.75E-09	0	1787	2188	1.00E+00	3.00E+00	2.88E+00	1.00E+00
5.80E+04	8.00E-03	0.00E+00	2.128E-07	-6.87E-09	0	1818	2208	1.00E+00	3.00E+00	2.88E+00	1.00E+00
5.90E+04	8.00E-03	0.00E+00	2.165E-07	-6.99E-09	0	1849	2228	1.00E+00	3.00E+00	2.88E+00	1.00E+00
6.00E+04	8.00E-03	0.00E+00	2.202E-07	-7.11E-09	0	1880	2248	1.00E+00	3.00E+00	2.88E+00	1.00E+00
6.10E+04	8.00E-03	0.00E+00	2.239E-07	-7.23E-09	0	1911	2268	1.00E+00	3.00E+00	2.88E+00	1.00E+00
6.20E+04	8.00E-03	0.00E+00	2.276E-07	-7.35E-09	0	1942	2288	1.00E+00	3.00E+00	2.88E+00	1.00E+00
6.30E+04	8.00E-03	0.00E+00	2.313E-07	-7.47E-09	0	1973	2308	1.00E+00	3.00E+00	2.88E+00	1.00E+00
6.40E+04	8.00E-03	0.00E+00	2.350E-07	-7.59E-09	0	2004	2328	1.00E+00	3.00E+00	2.88E+00	1.00E+00
6.50E+04	8.00E-03	0.00E+00	2.387E-07	-7.71E-09	0	2035	2348	1.00E+00	3.00E+00	2.88E+00	1.00E+00
6.60E+04	8.00E-03	0.00E+00	2.424E-07	-7.83E-09	0	2066	2368	1.00E+00	3.00E+00	2.88E+00	1.00E+00
6.70E+04	8.00E-03	0.00E+00	2.461E-07	-7.95E-09	0	2097	2388	1.00E+00	3.00E+00	2.88E+00	1.00E+00
6.80E+04	8.00E-03	0.00E+00	2.498E-07	-8.07E-09	0	2128	2408	1.00E+00	3.00E+00	2.88E+00	1.00E+00
6.90E+04	8.00E-03	0.00E+00	2.535E-07	-8.19E-09	0	2159	2428	1.00E+00	3.00E+00	2.88E+00	1.00E+00
7.00E+04	8.00E-03	0.00E+00	2.572E-07	-8.31E-09	0	2190	2448	1.00E+00	3.00E+00	2.88E+00	1.00E+00
7.10E+04	8.00E-03	0.00E+00	2.609E-07	-8.43E-09	0	2221	2468	1.00E+00	3.00E+00	2.88E+00	1.00E+00
7.20E+04	8.00E-03	0.00E+00	2.646E-07	-8.55E-09	0	2252	2488	1.00E+00	3.00E+00	2.88E+00	1.00E+00
7.30E+04	8.00E-03	0.00E+00	2.683E-07	-8.67E-09	0	2283	2508	1.00E+00	3.00E+00	2.88E+00	1.00E+00
7.40E+04	8.00E-03	0.00E+00	2.720E-07	-8.79E-09	0	2314	2528	1.00E+00	3.00E+00	2.88E+00	1.00E+00
7.50E+04	8.00E-03	0.00E+00	2.757E-07	-8.91E-09	0	2345	2548	1.00E+00	3.00E+00	2.88E+00	1.00E+00
7.60E+04	8.00E-03	0.00E+00	2.794E-07	-9.03E-09	0	2376	2568	1.00E+00	3.00E+00	2.88E+00	1.00E+00
7.70E+04	8.00E-03	0.00E+00	2.831E-07	-9.15E-09	0	2407	2588	1.00E+00	3.00E+00	2.88E+00	1.00E+00
7.80E+04	8.00E-03	0.00E+00	2.868E-07	-9.27E-09	0	2438	2608	1.00E+00	3.00E+00	2.88E+00	1.00E+00
7.90E+04	8.00E-03	0.00E+00	2.905E-07	-9.39E-09	0	2469	2628	1.00E+00	3.00E+00	2.88E+00	1.00E+00
8.00E+04	8.00E-03	0.00E+00	2.942E-07	-9.51E-09	0	2500	2648	1.00E+00	3.00E+00	2.88E+00	1.00E+00
8.10E+04	8.00E-03	0.00E+00	2.979E-07	-9.63E-09	0	2531	2668	1.00E+00	3.00E+00	2.88E+00	1.00E+00
8.20E+04	8.00E-03	0.00E+00	3.016E-07	-9.75E-09	0	2562	2688	1.00E+00</td			

Gerya (2019)

Visualize output and
record analytical
procedures in
Python.



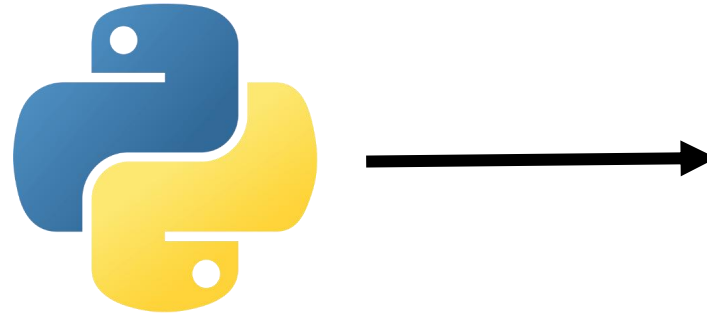
Quantify ASPECT
model observation
(e.g., continental
fragment width)

Automated data analysis

Model output

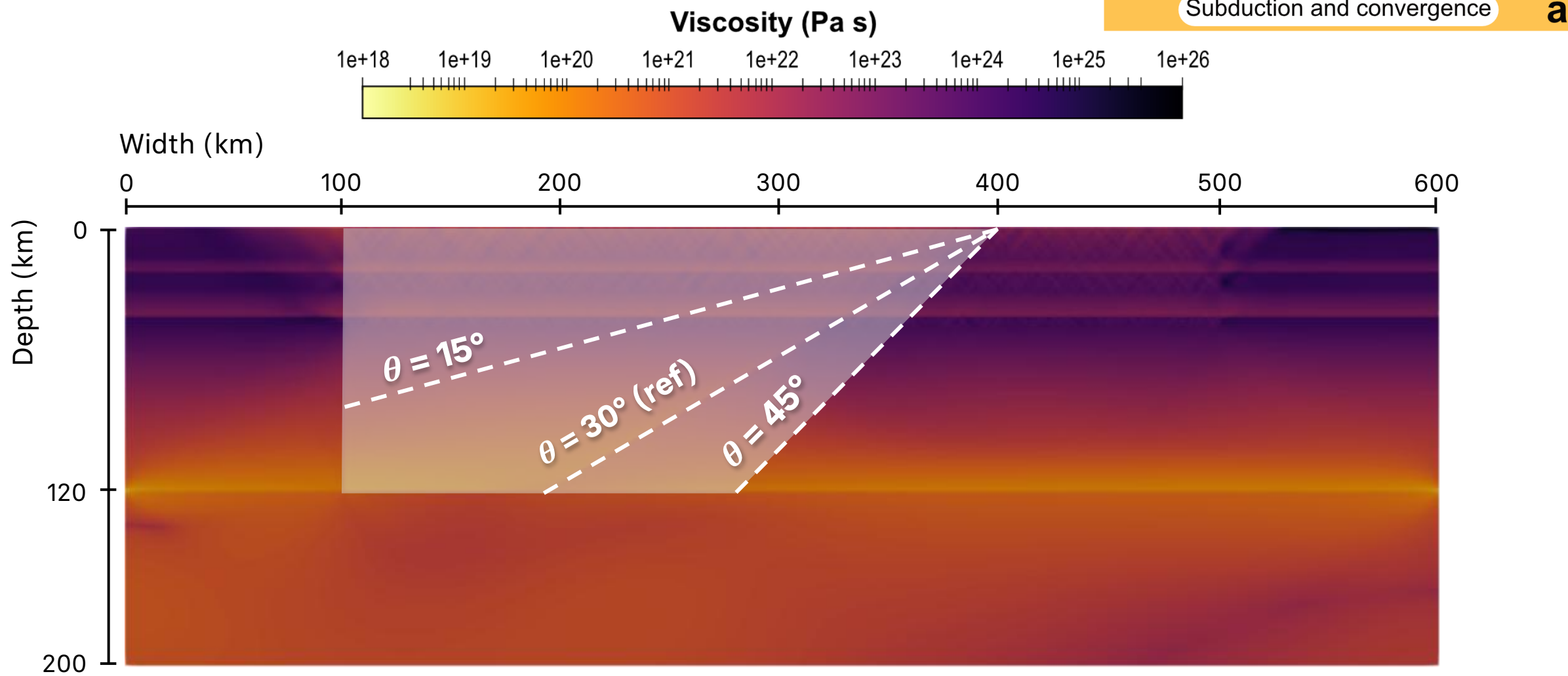
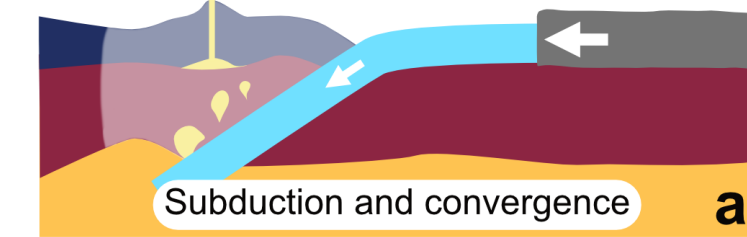
solution-00000.0000.vtu
solution-00000.pvtu
solution-00001.0000.vtu
solution-00001.pvtu
solution-00002.0000.vtu
solution-00002.pvtu
solution-00002.0000.vtu
solution-00003.pvtu
solution-00003.0000.vtu
solution-00004.pvtu
solution-00004.0000.vtu
...

The power of
for loops



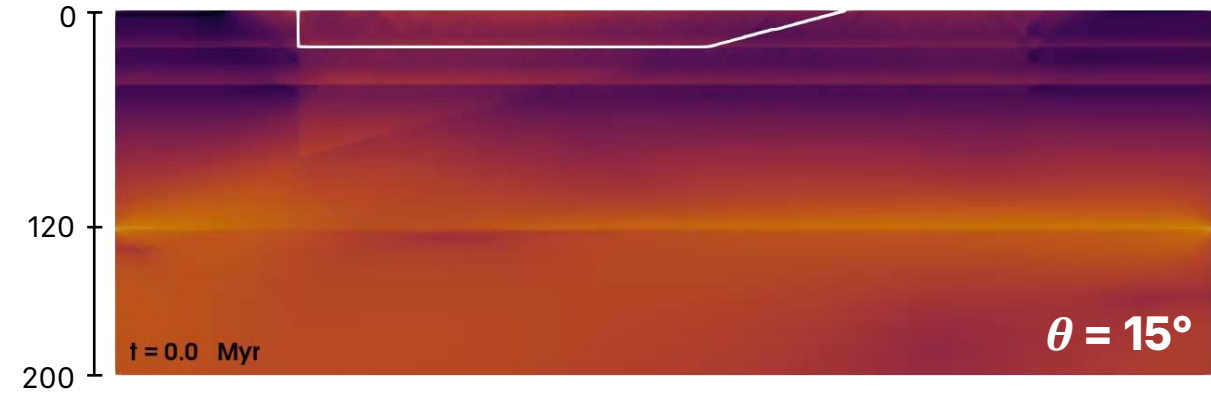
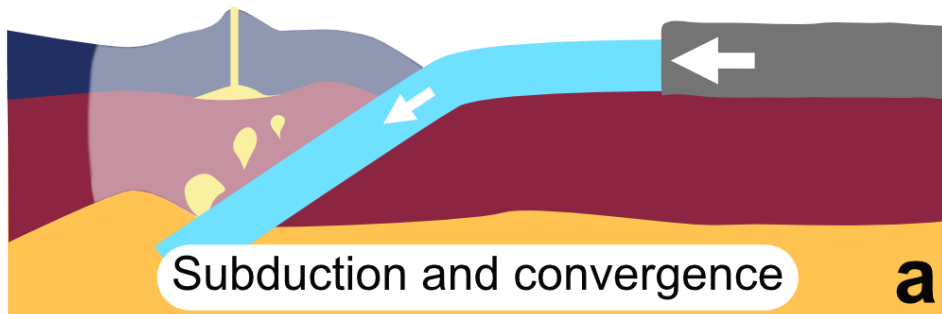
Over 90% reduction in
time of analysis vs
manual measurements.
Consistent results.

Dip angle of old suture



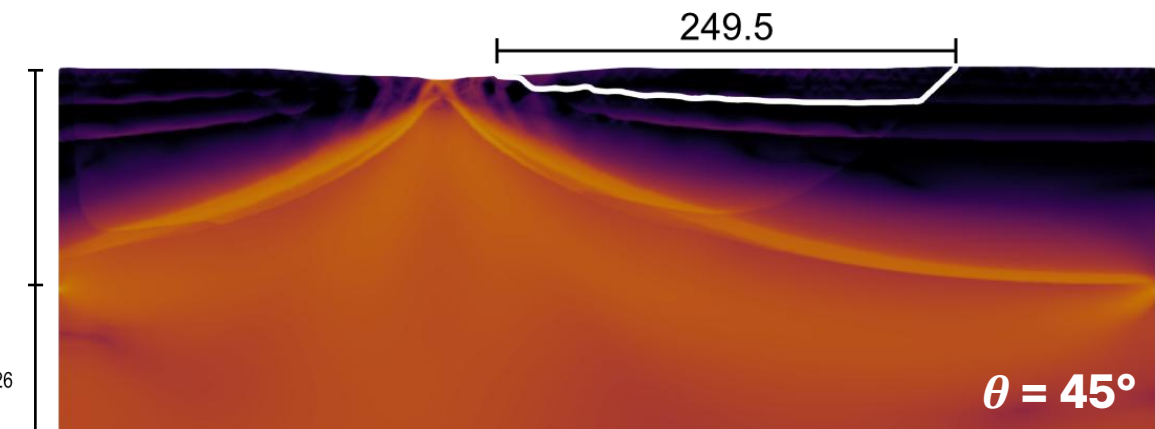
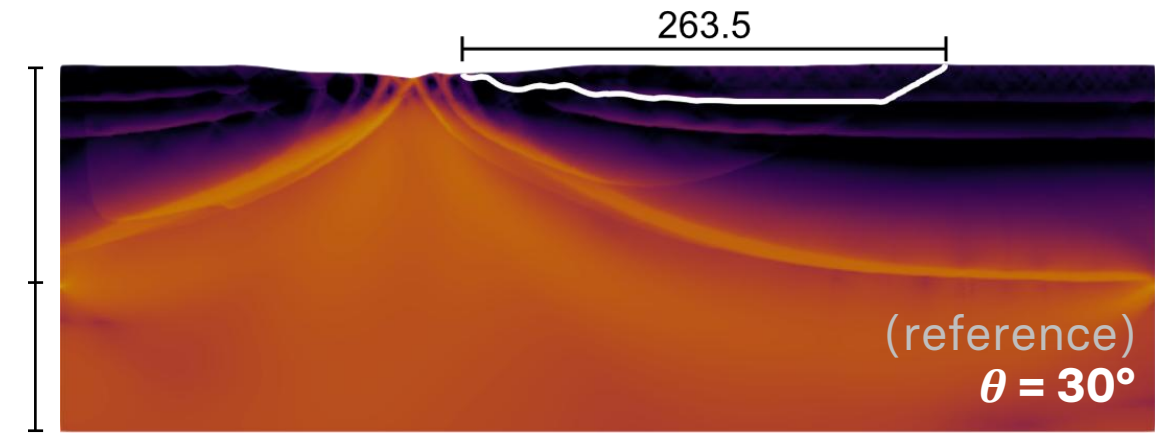
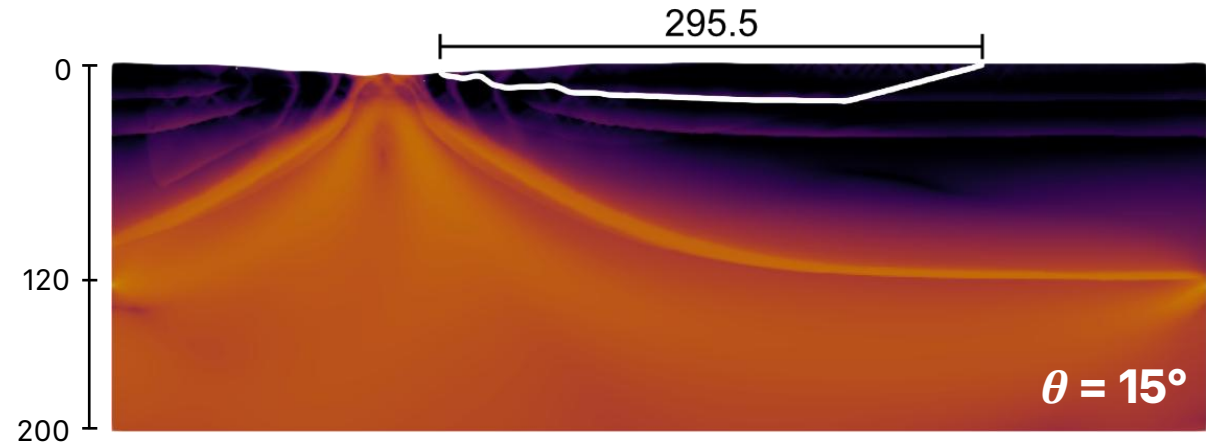
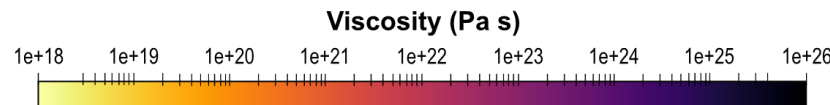
Dip angle of old suture

Geometry of subduction-related rheological weakness



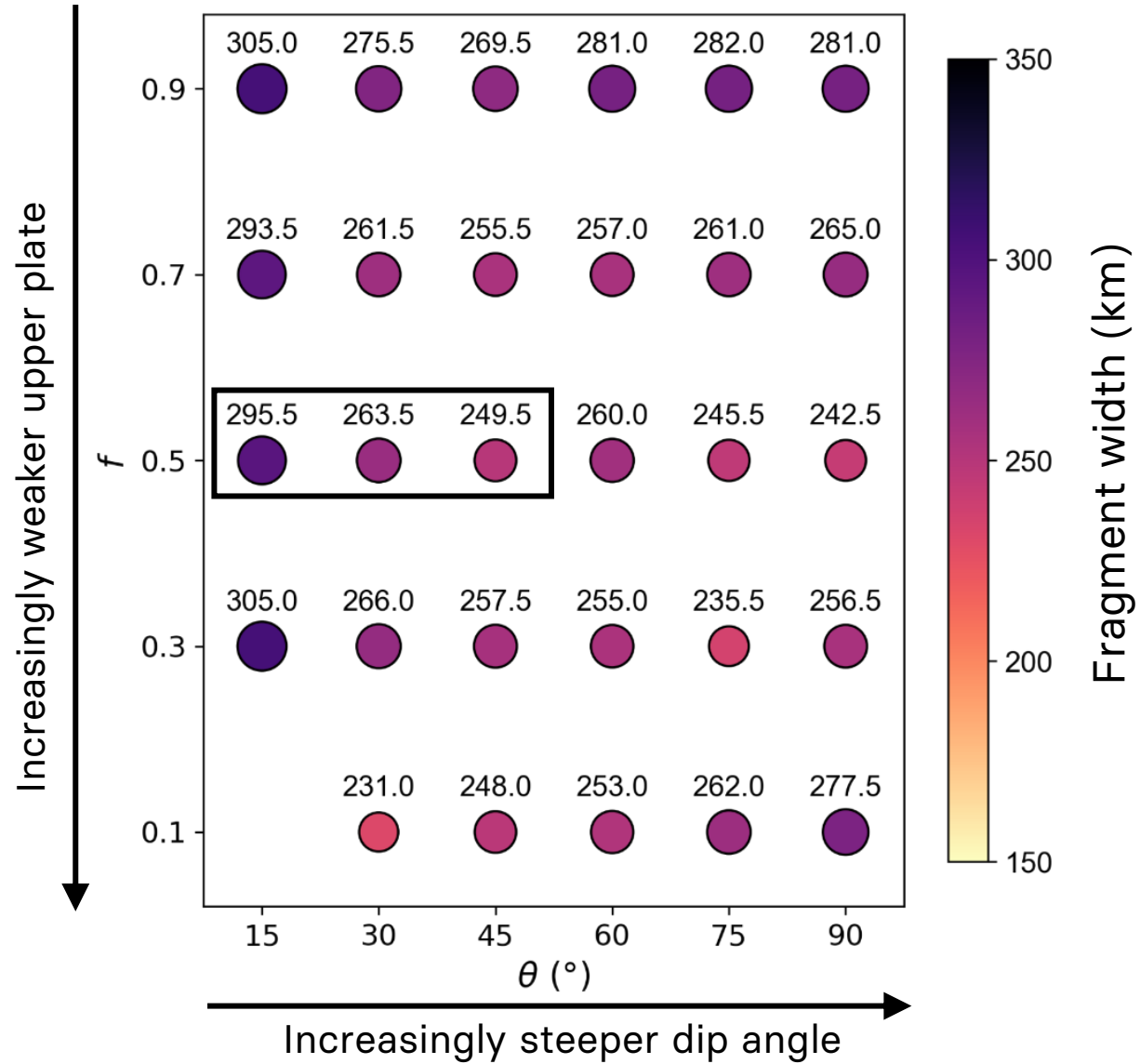
Dip angle of old suture

- $\theta = 15^\circ - 45^\circ$: a **steeper** dip angle creates a **smaller** fragment

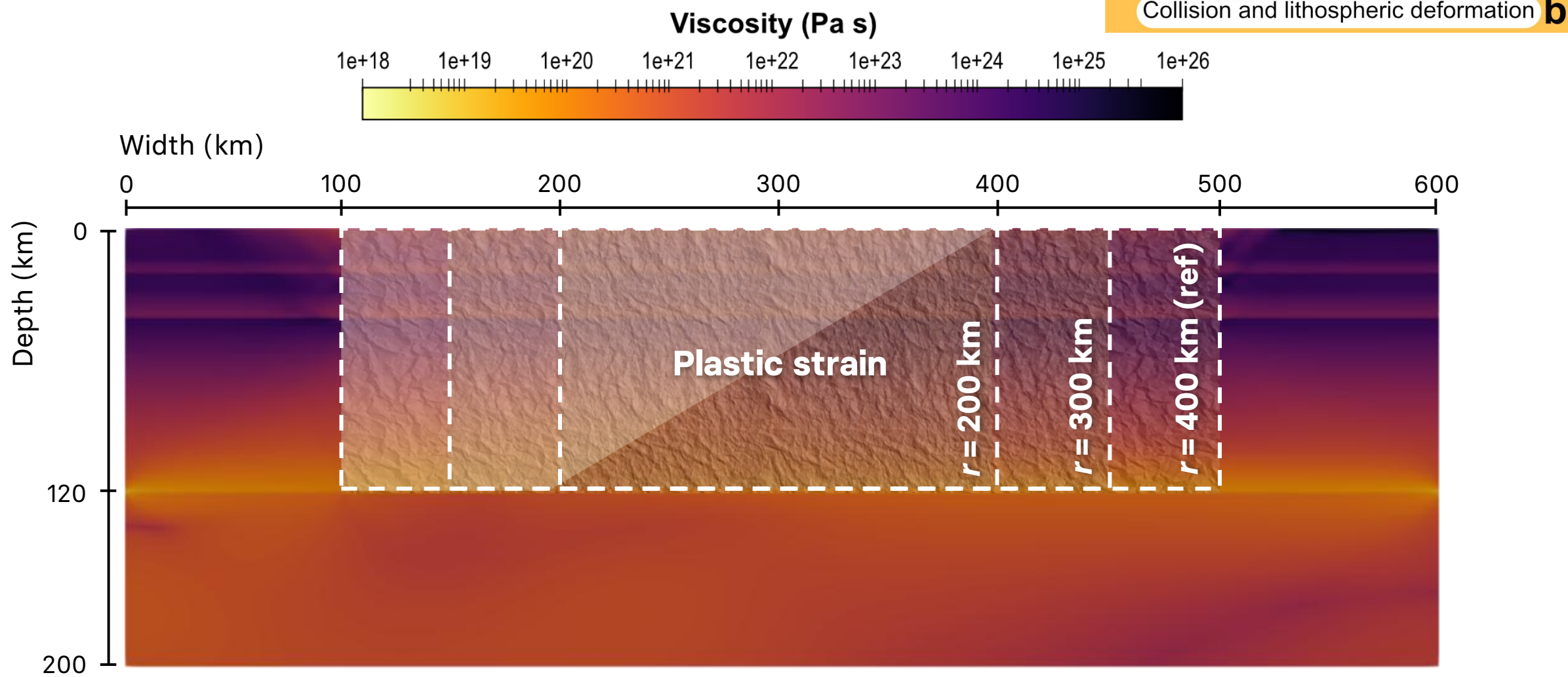


Dip angle of old suture

- $\vartheta = 15^\circ - 45^\circ$: a **steeper** dip angle creates a **smaller** fragment
- $\vartheta = 60^\circ - 90^\circ$: more **random** variations in fragment widths
- $f = 0.1$: a steeper dip angle, however, creates a larger fragment.



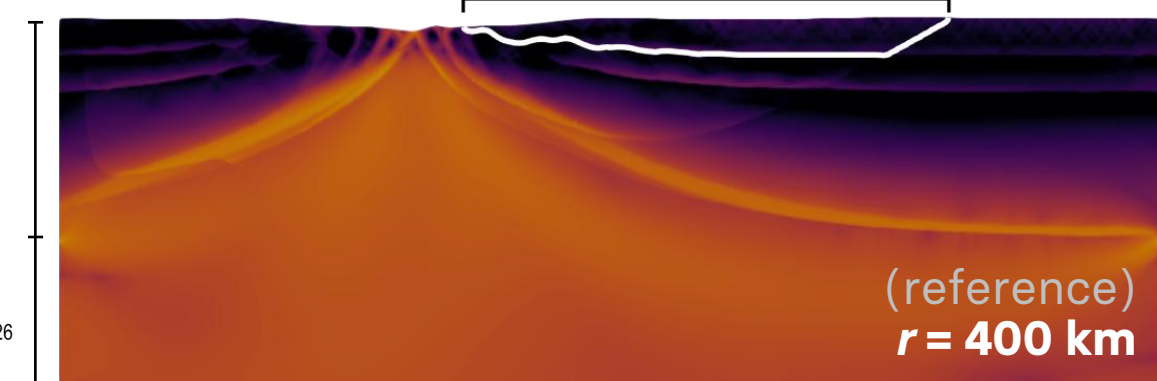
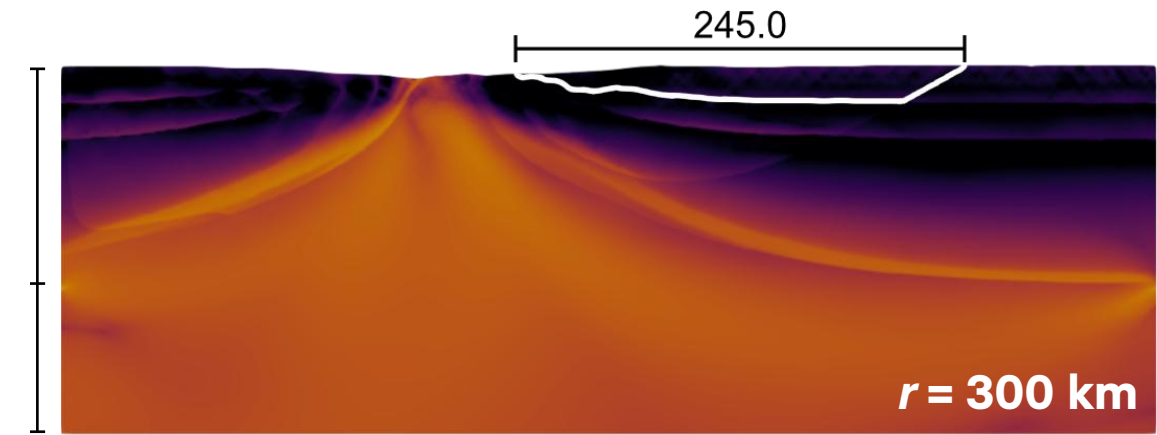
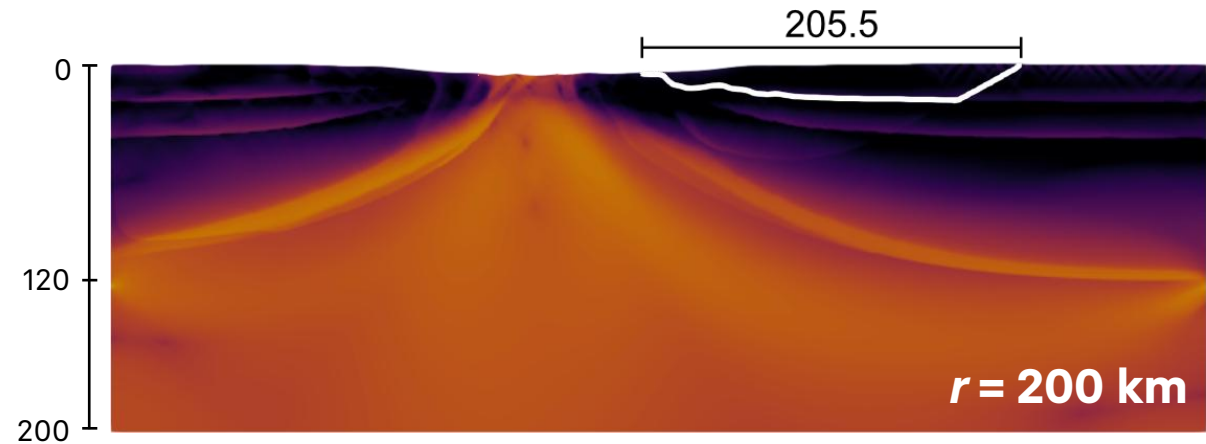
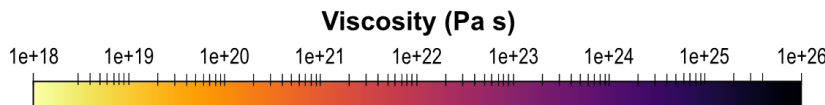
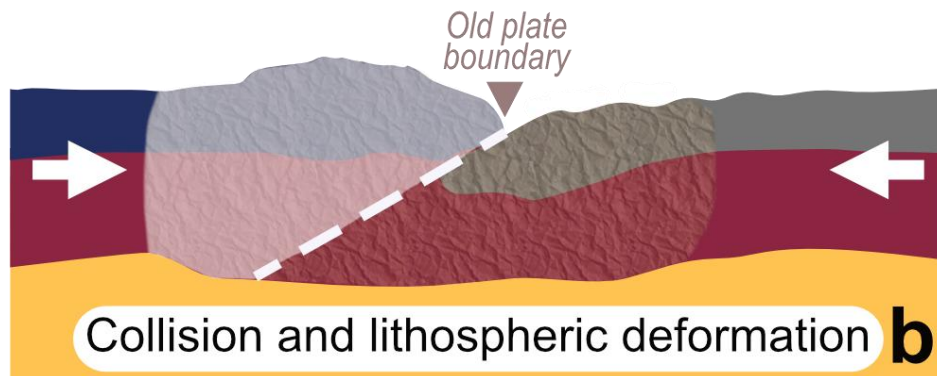
Extent of orogenic deformation



Extent of orogeny

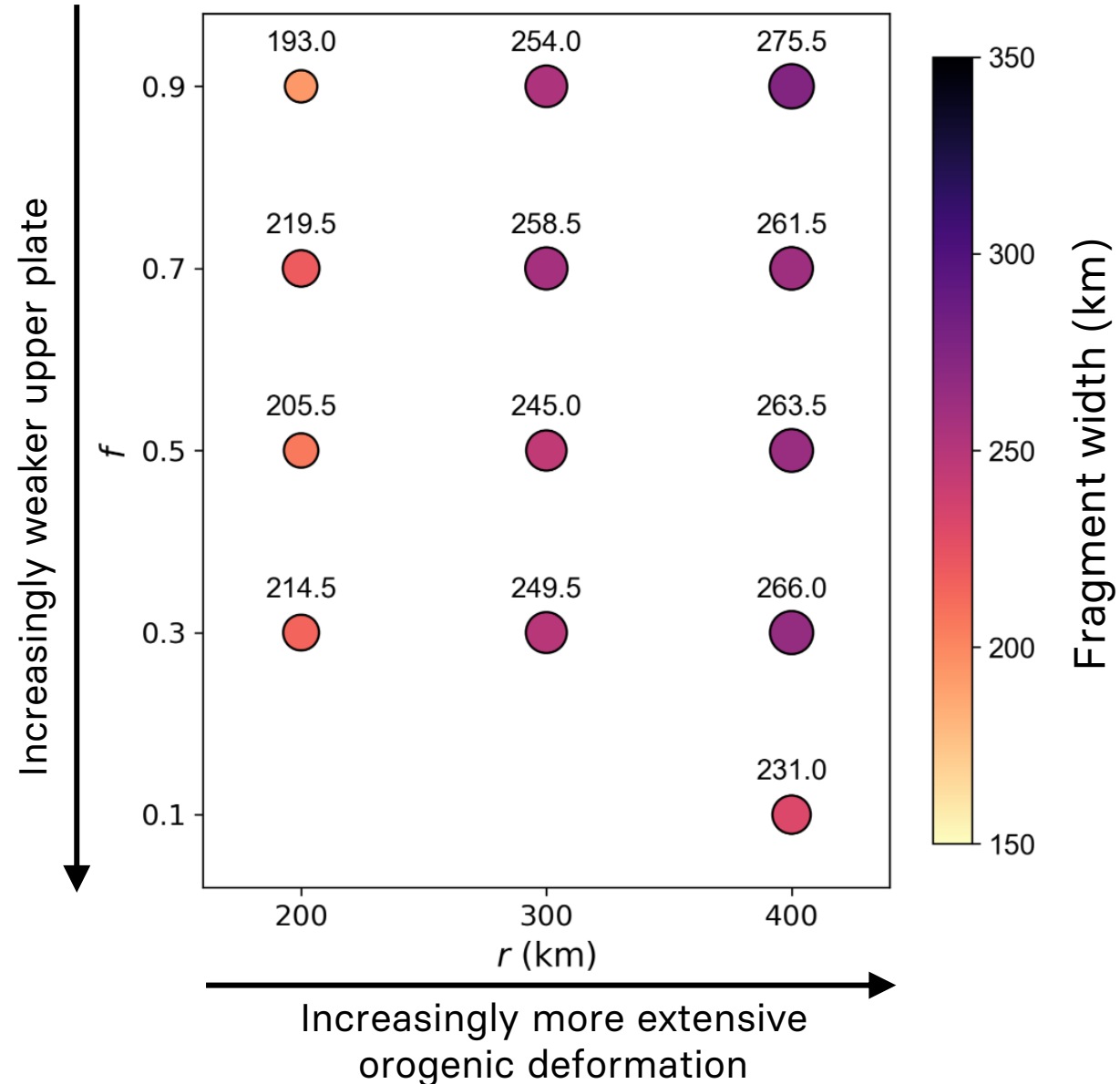
- A **more extensive** deformation zone creates a **larger** fragment.

Geometry of orogenesis-related strain weakness

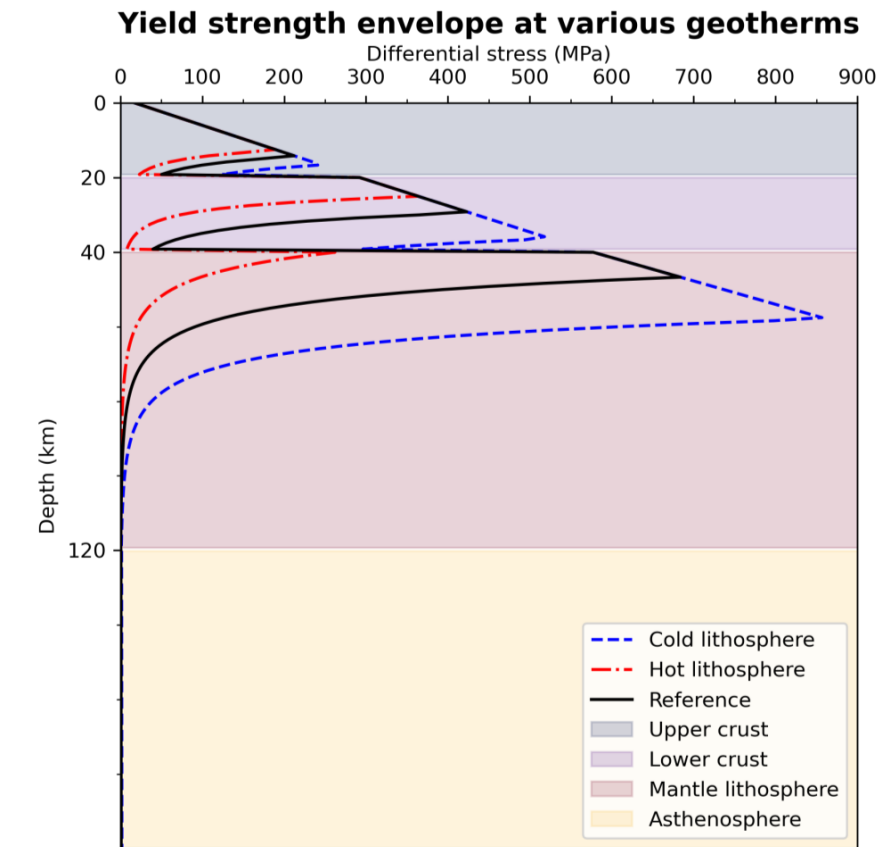
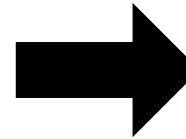
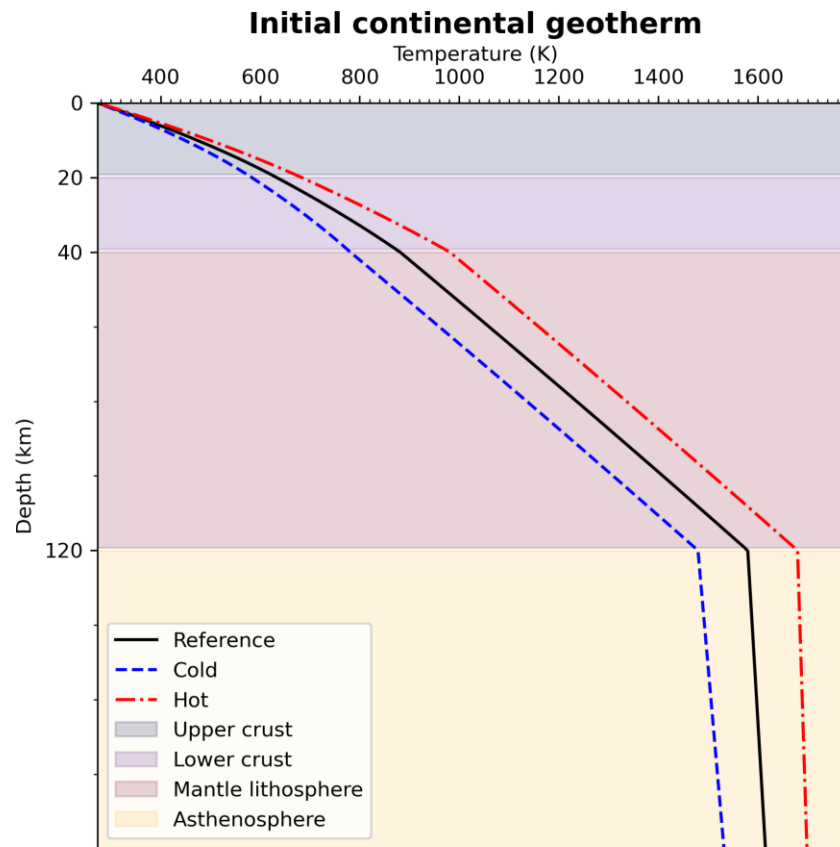


Extent of orogeny

- **More extensive** orogenic deformation creates a **larger** fragment.
- $f = 0.1$: some models fail due to the nonlinearity of ductile deformation.

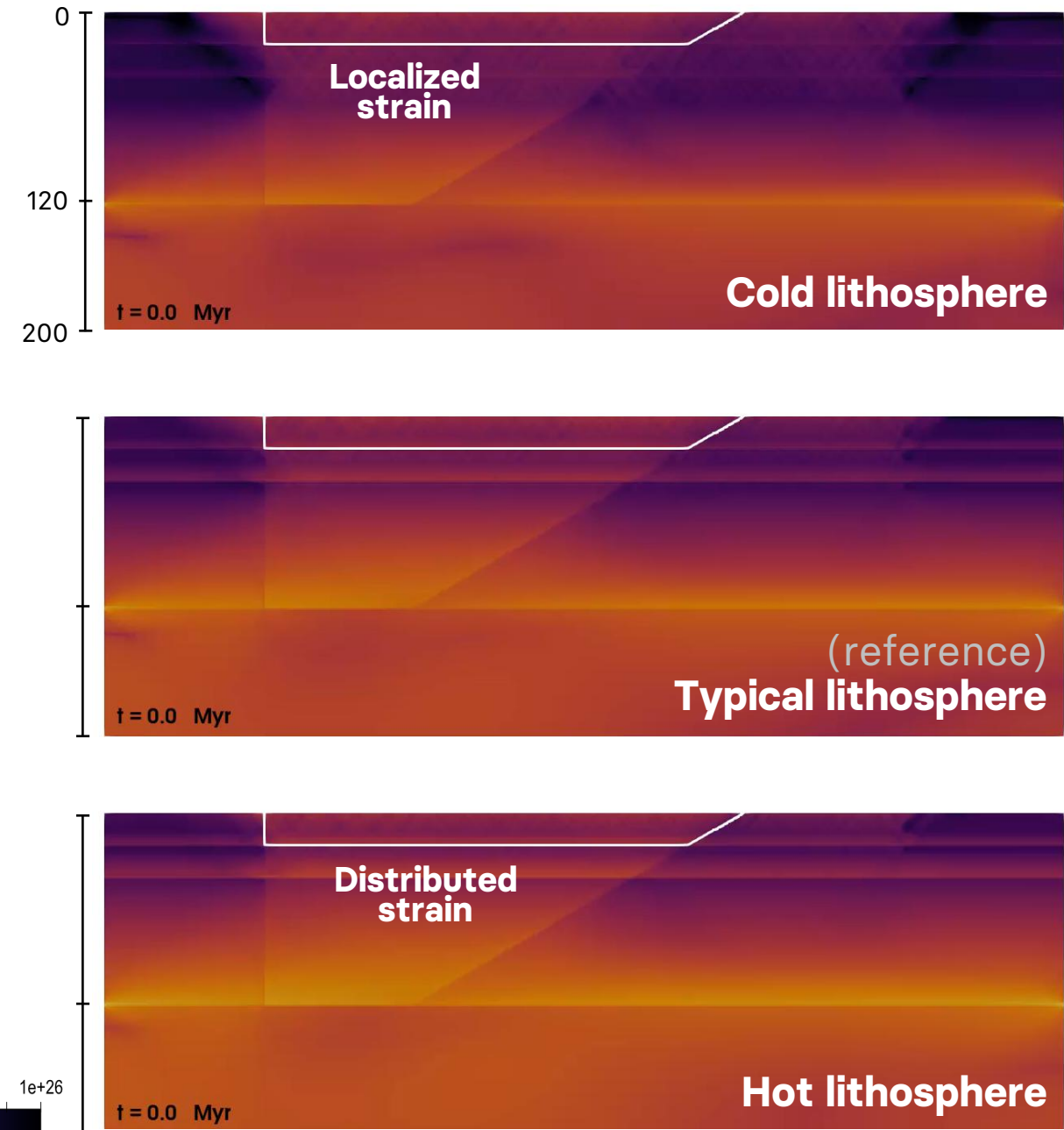
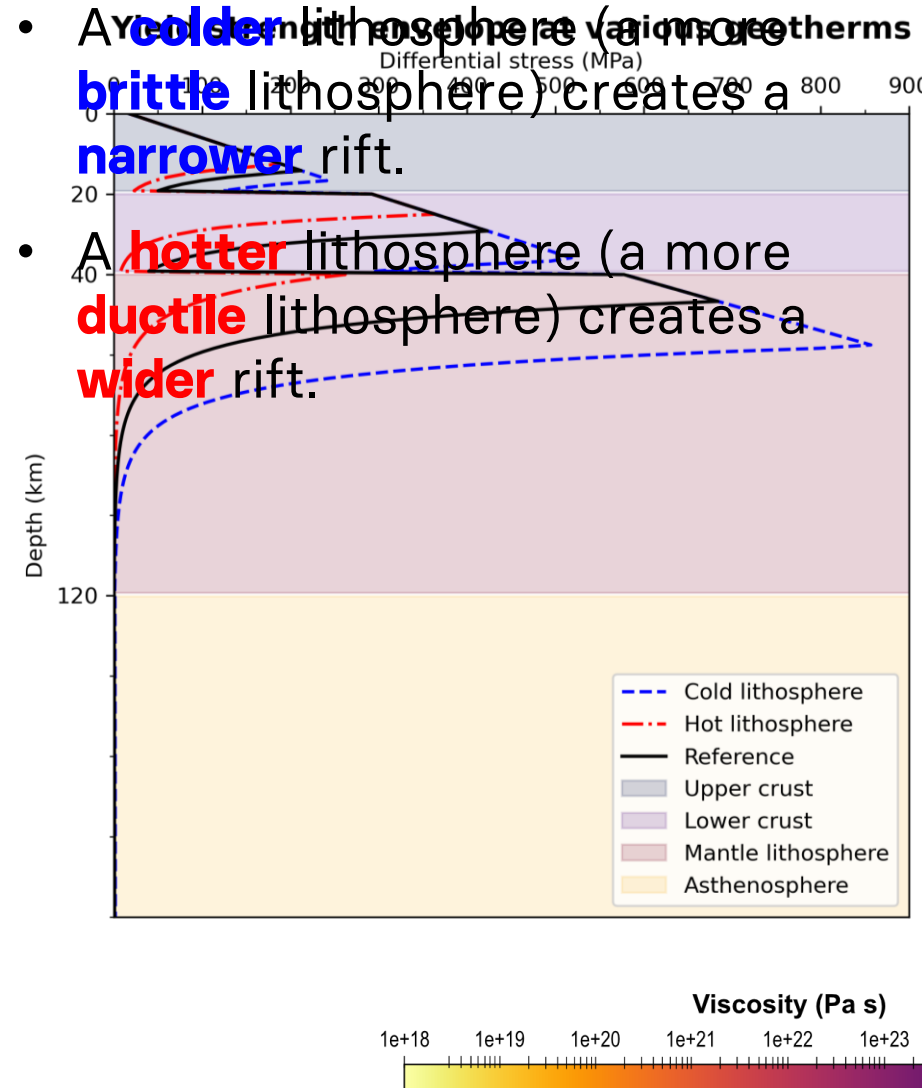


Initial model geotherm



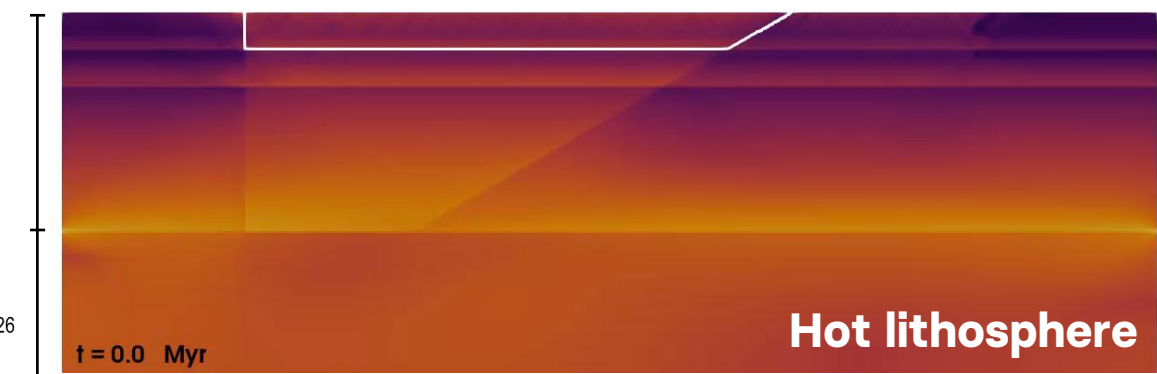
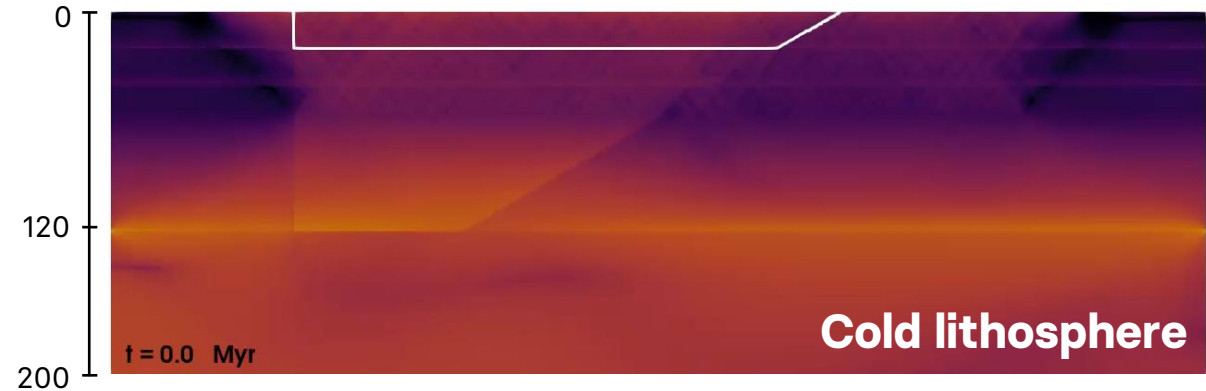
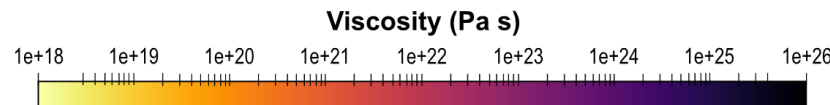
- The initial geotherm changes the **brittle-ductile transition** depth.
- A **colder** geotherm leads to a more **brittle** lithosphere.
- A **hotter** geotherm leads to a more **ductile** lithosphere.

Initial model geotherm

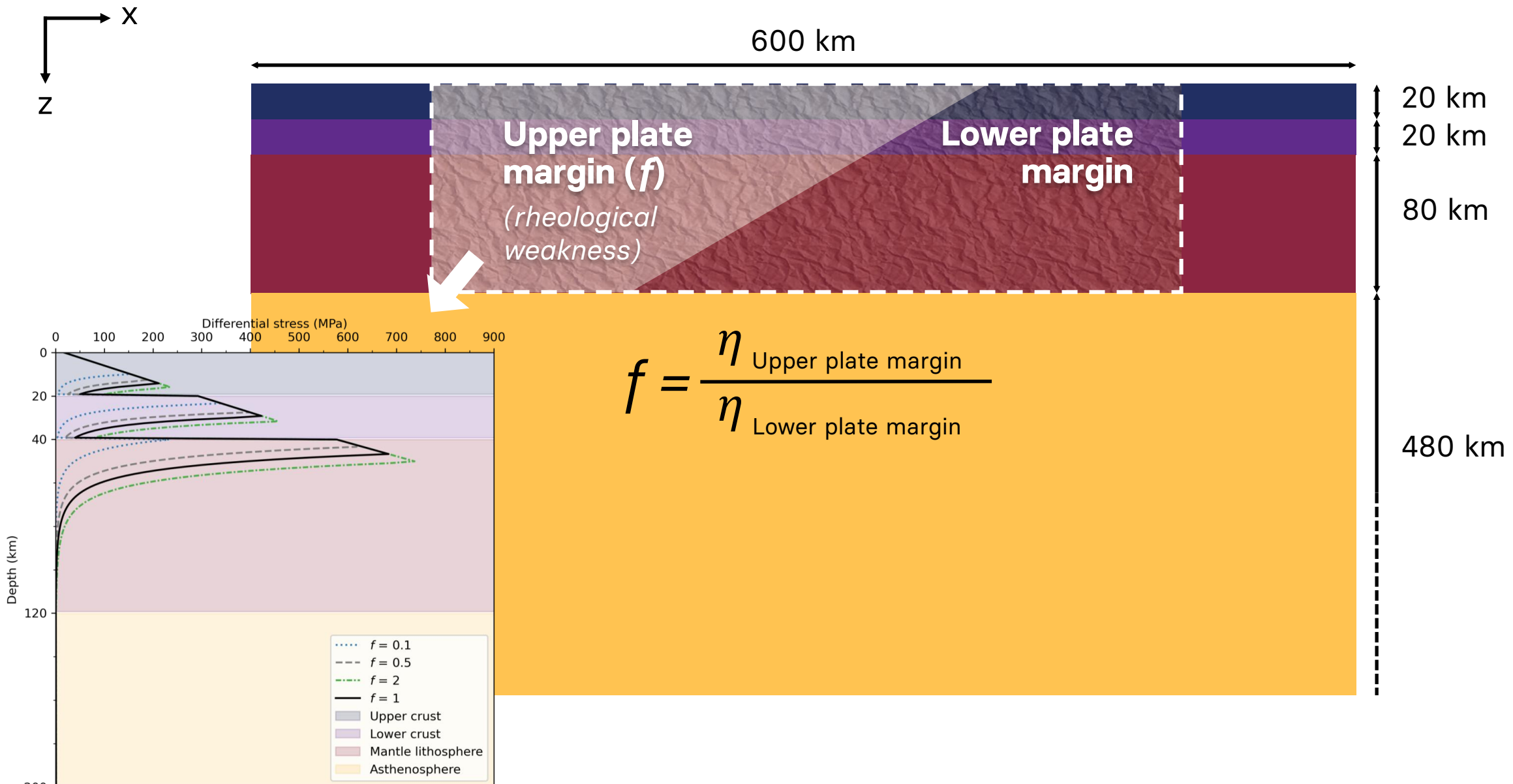


Initial model geotherm

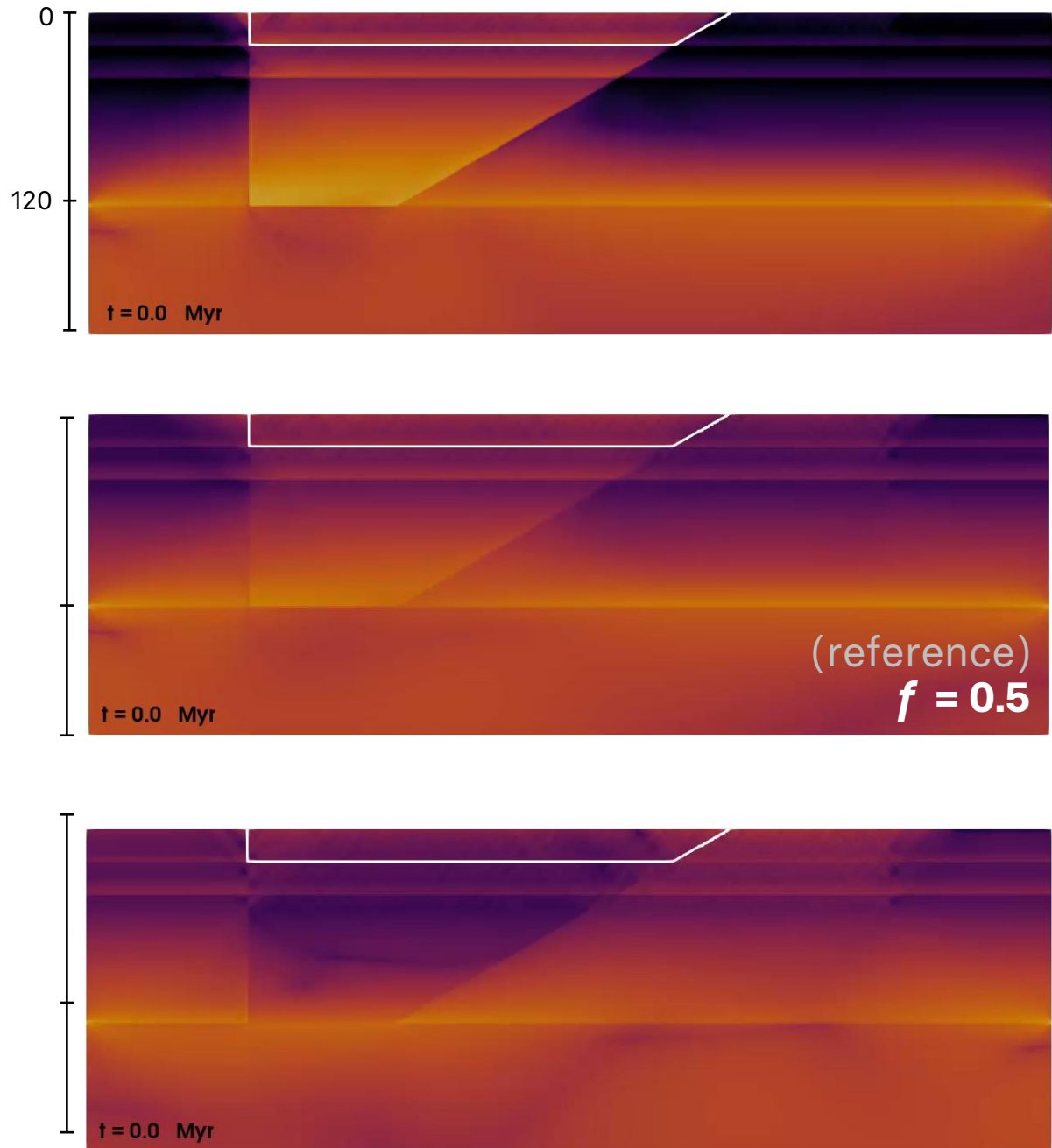
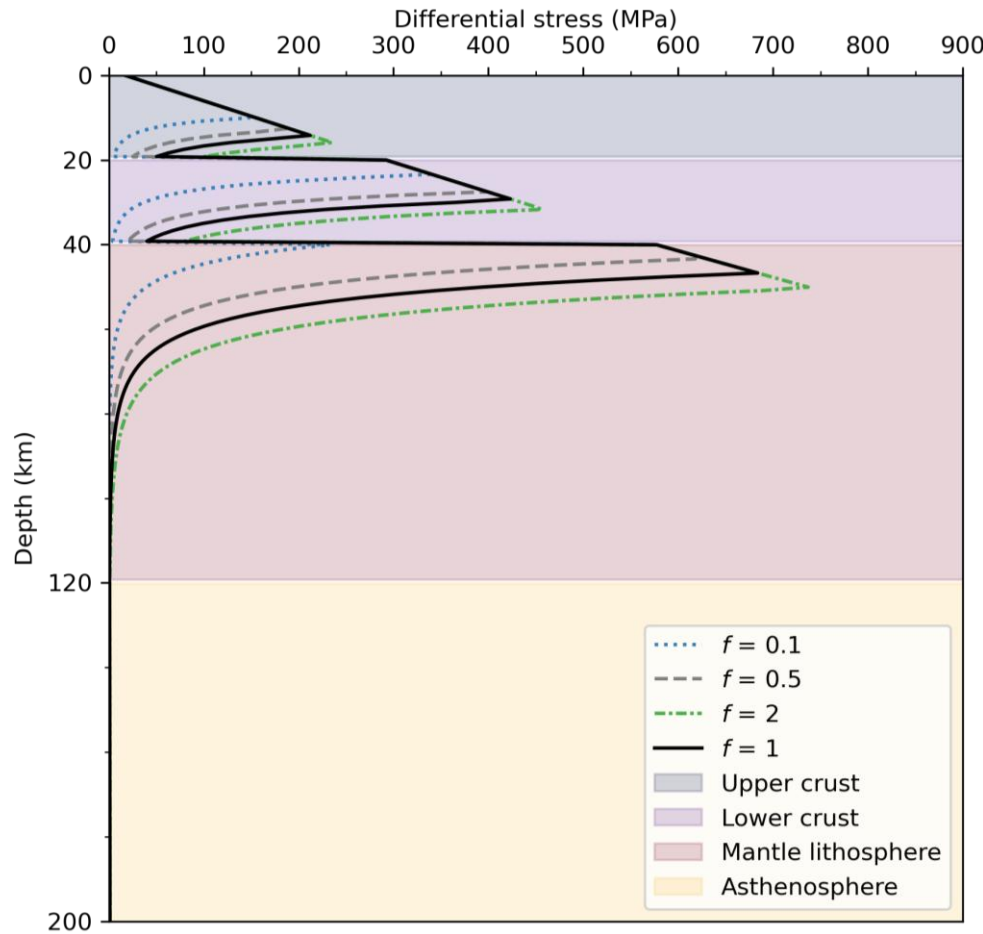
- A **colder** lithosphere (a more **brittle** lithosphere) creates a **narrower** rift.
- A **hotter** lithosphere (a more **ductile** lithosphere) creates a **wider** rift.
- The initial geotherm influences **strain localization** during rifting.



Strength parameter

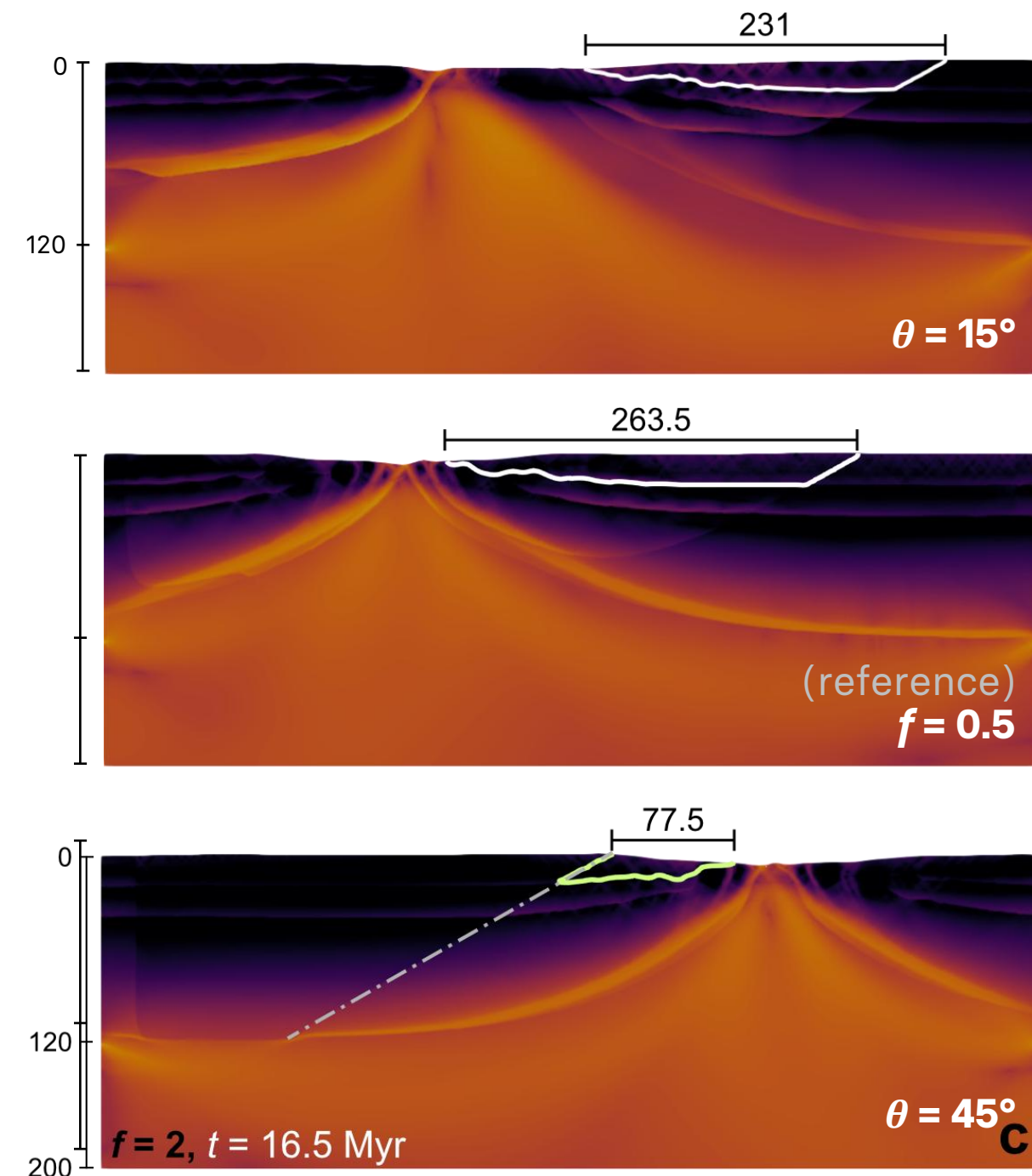
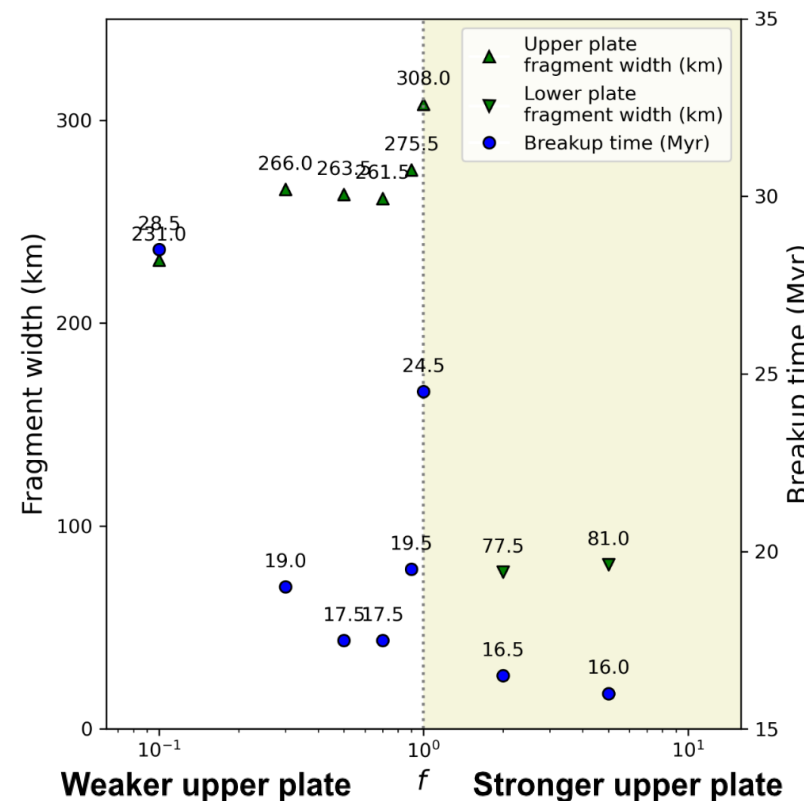


Strength parameter



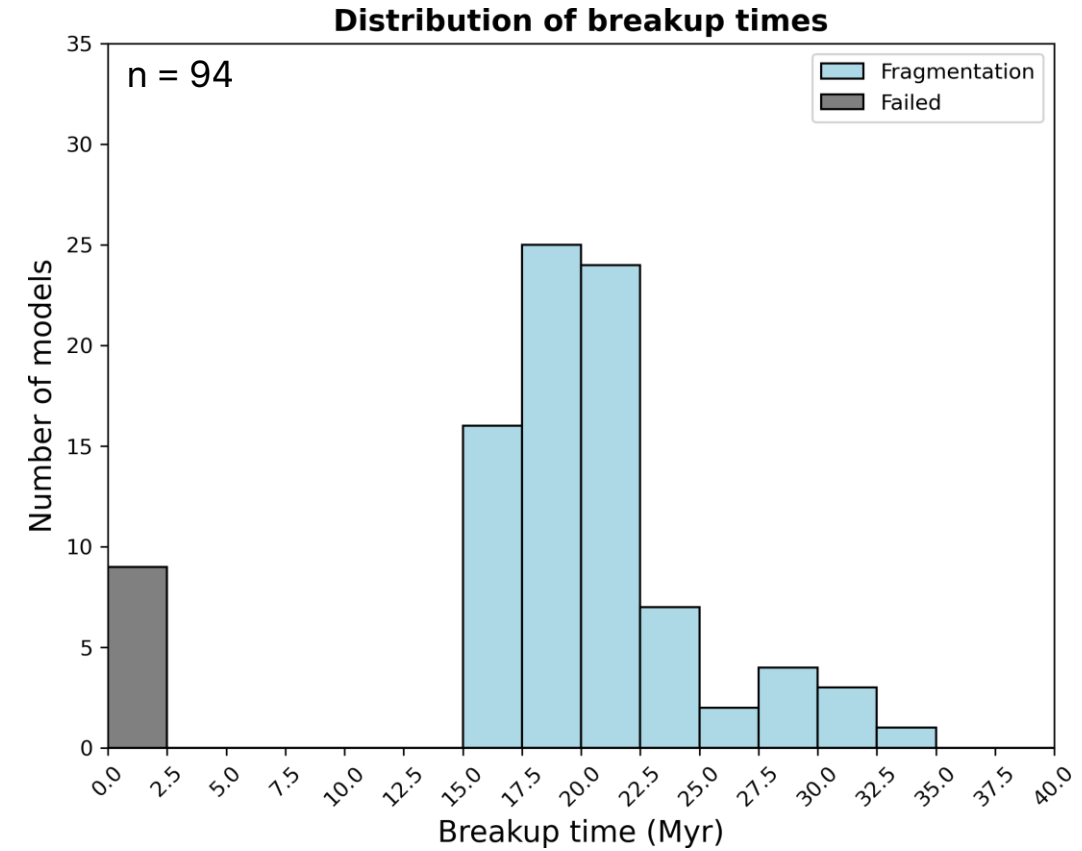
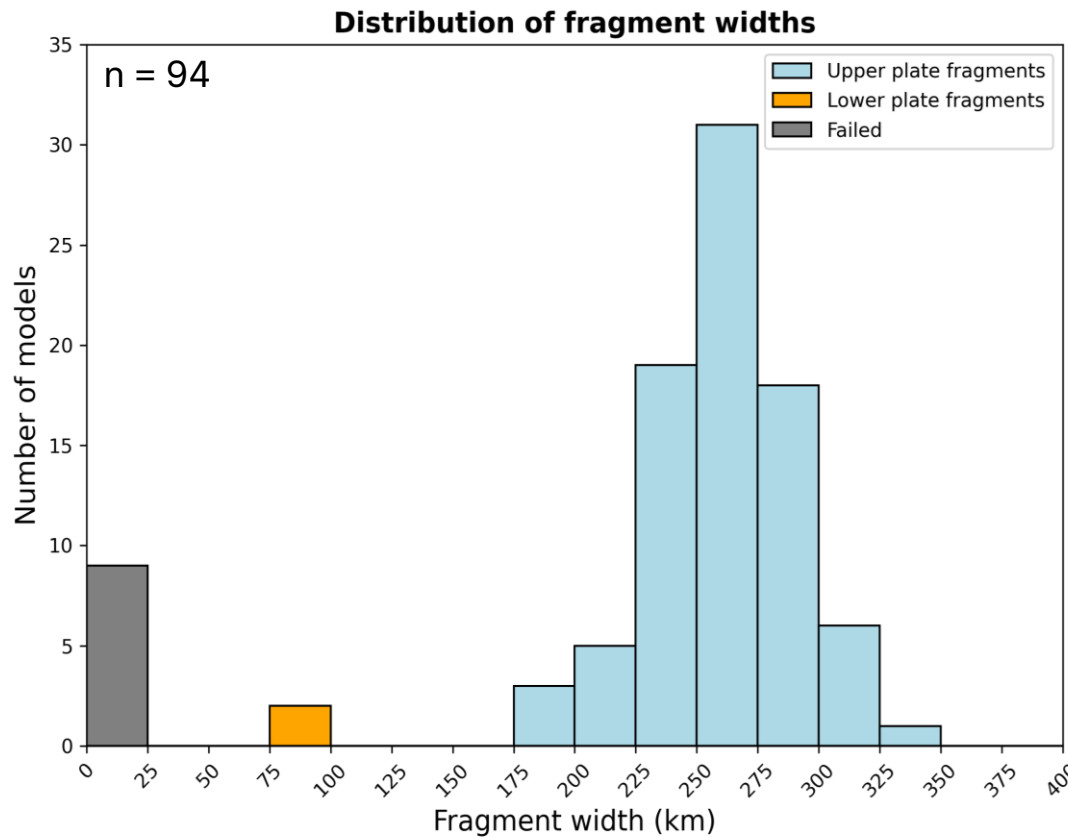
Strength parameter

- $f = 0.1$ - delocalized thinning and a wider rift.
- $f > 1$ - fragment instead forms in lower plate.
- Rifts tend to exploit **relatively weaker** areas.



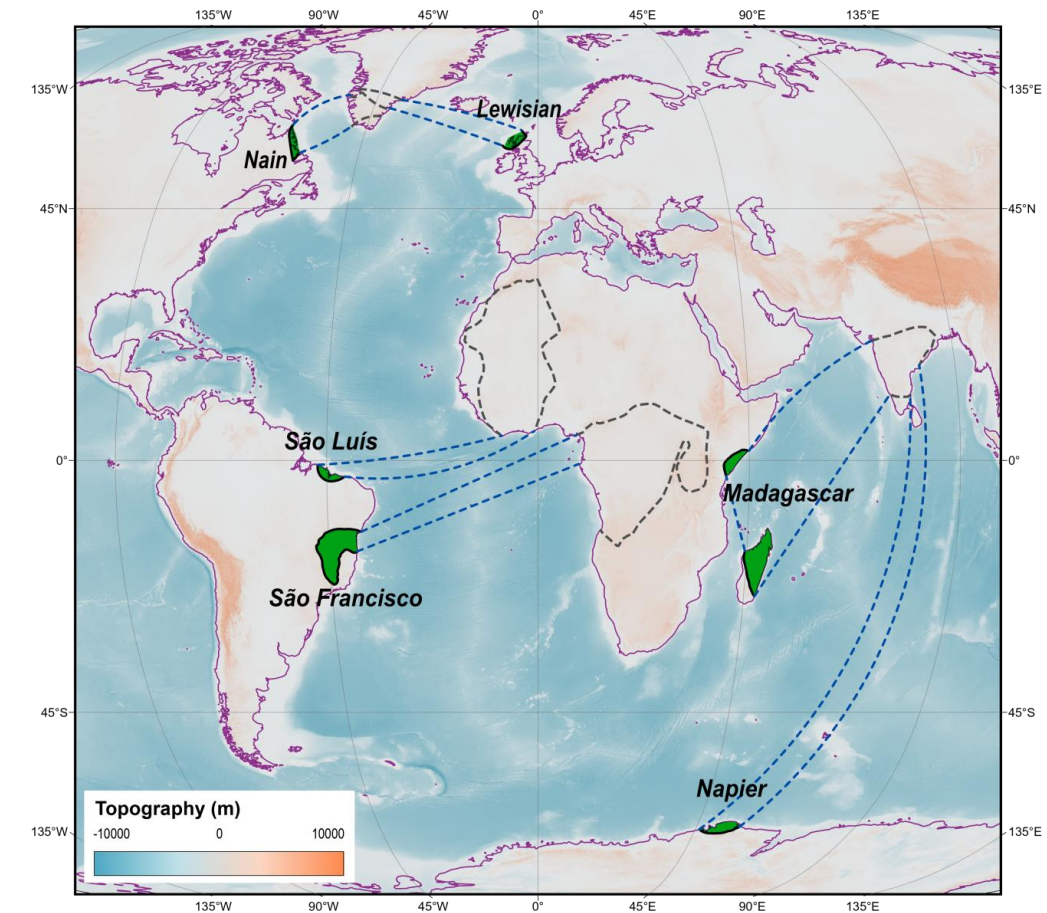
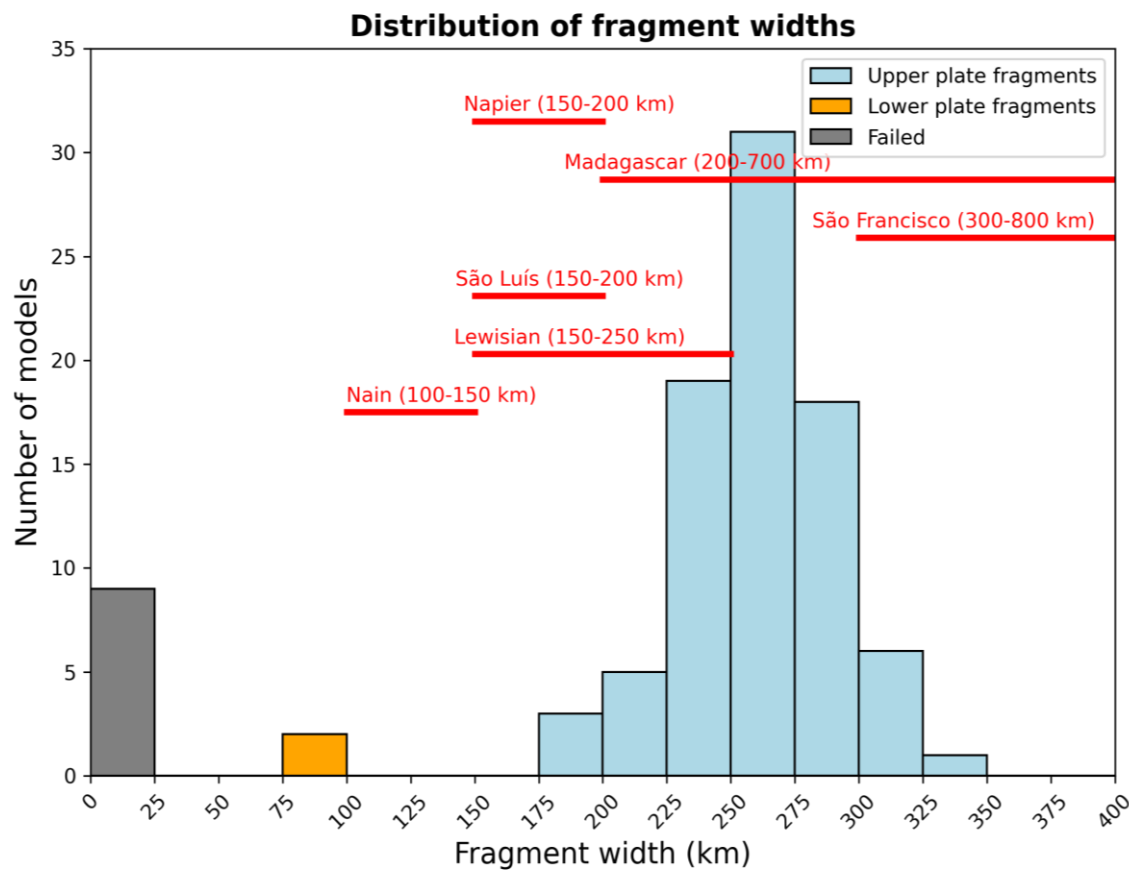
Model summary

- By testing 8 parameters, we produce fragments in widths of **~175–350 km** over **~15–35 Myr.**



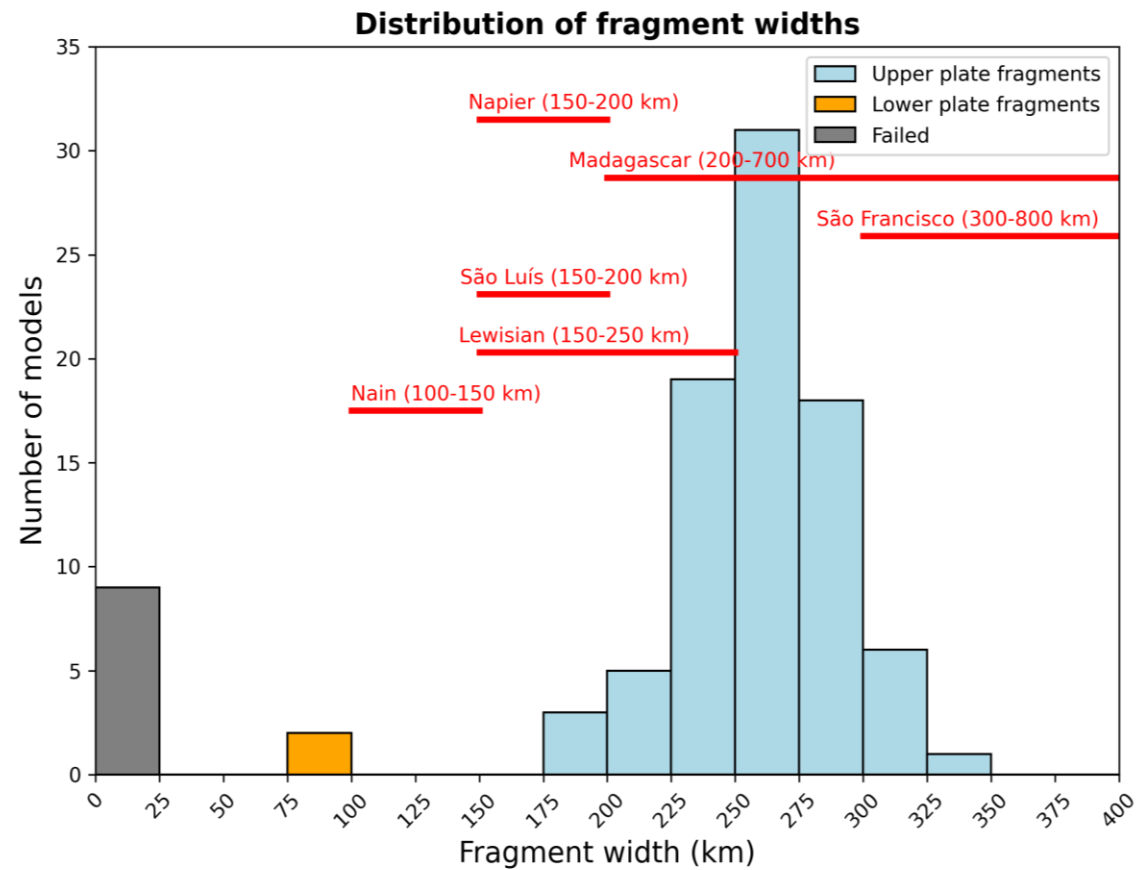
Comparison with geological examples

- Our modelled fragment widths align with many geological examples.
 - All examples above experienced **several episodes of Wilson Cycles**.



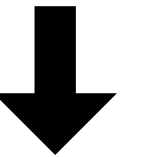
Conclusions

- Using an automated system, we quantify the **influence of structural inheritance** in fragment formation.
- The **geometry of inherited structures** directly controls the fragment width.
- However, the rift process can also be influenced by the **initial geotherm** (and other factors).
- Our modelled fragments **align with many geological examples**.
- We provide a **tectonic recipe** for future regional models.



Thank you!

Access to setup, tutorial, code, and data



github.com/alanjyu/fragment_recipe



Governing equations

$$\nabla \cdot \mathbf{u} = 0$$

Mass

$$-\nabla \cdot \mu \dot{\varepsilon}(\mathbf{u}) + \nabla P = \rho \mathbf{g}$$

Linear momentum

$$\rho C_p \left(\frac{\partial T}{\partial t} + \mathbf{u} \cdot \nabla T \right) - \nabla \cdot k \nabla T = \rho H$$

Energy

$$\rho = \rho_0 (1 - \alpha (T' - T_0'))$$

Equation of state

Boussinesq approximation

- The compressional Navier-Stokes equations are highly nonlinear and unstable.
- $\frac{\Delta\rho}{\rho} \ll 1$, density variation not considered except in the buoyancy term ρg
- Density is loosely related to temperature.

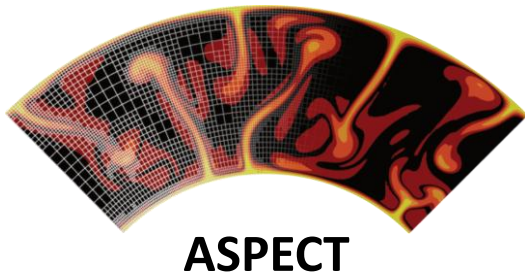
$$\rho = \rho_0(1 - \alpha(T' - T_0'))$$

where $\alpha = -\frac{1}{\rho_0} \left(\frac{\partial \rho}{\partial T}\right)_P$ is the thermal expansivity.

Infinite Prandtl Number

- $Pr = \frac{\text{momentum diffusivity}}{\text{thermal diffusivity}} \sim 10^{25}$ for Earth's mantle
- In physical terms, infinite Pr means that heat conduction is very slow compared to momentum diffusion.

Numerical modelling



Initial physical model

Forward model (in time)

Model output

$$\nabla \cdot \mathbf{u} = 0$$

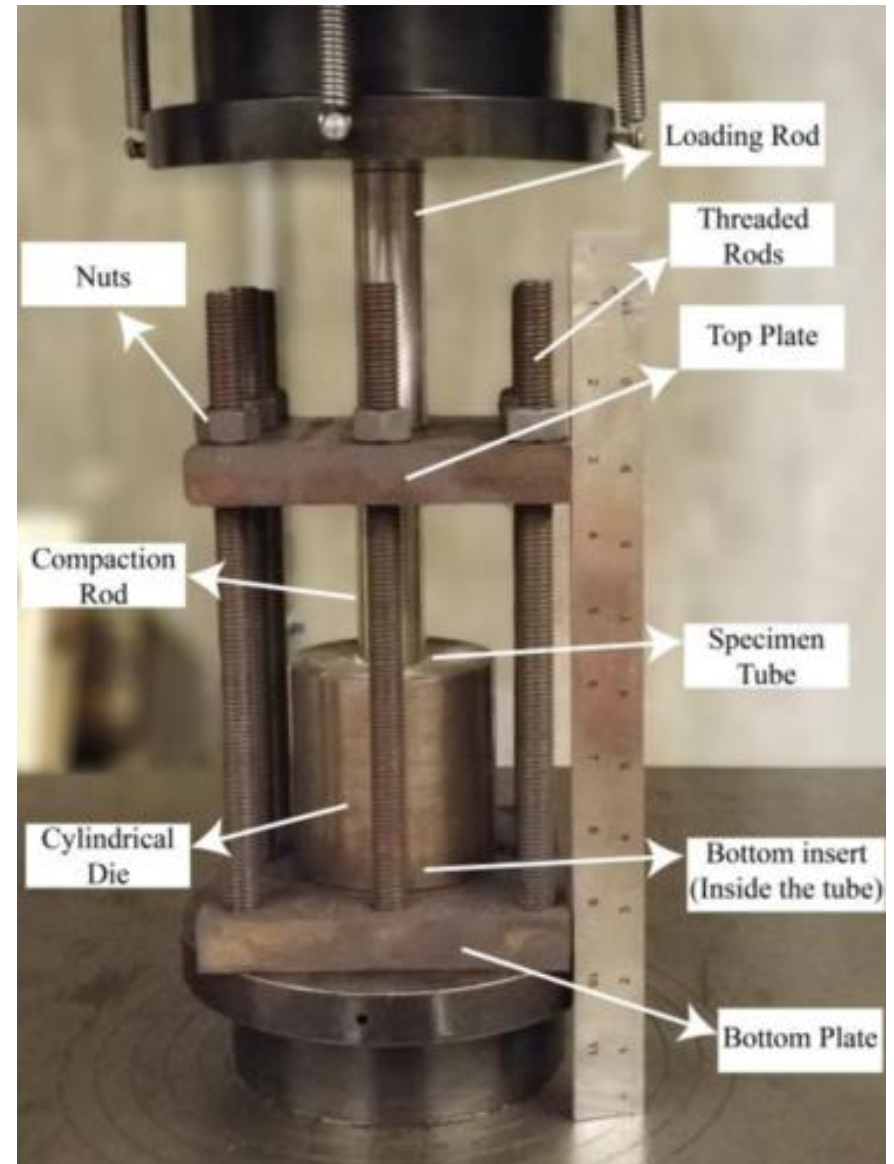
$$-\nabla \cdot \mu \dot{\varepsilon}(\mathbf{u}) + \nabla P = \rho \mathbf{g}$$

$$\rho C_p \left(\frac{\partial T}{\partial t} + \mathbf{u} \cdot \nabla T \right) - \nabla \cdot k \nabla T = \rho H$$

$$\rho = \rho_0 (1 - \alpha (T' - T_0'))$$

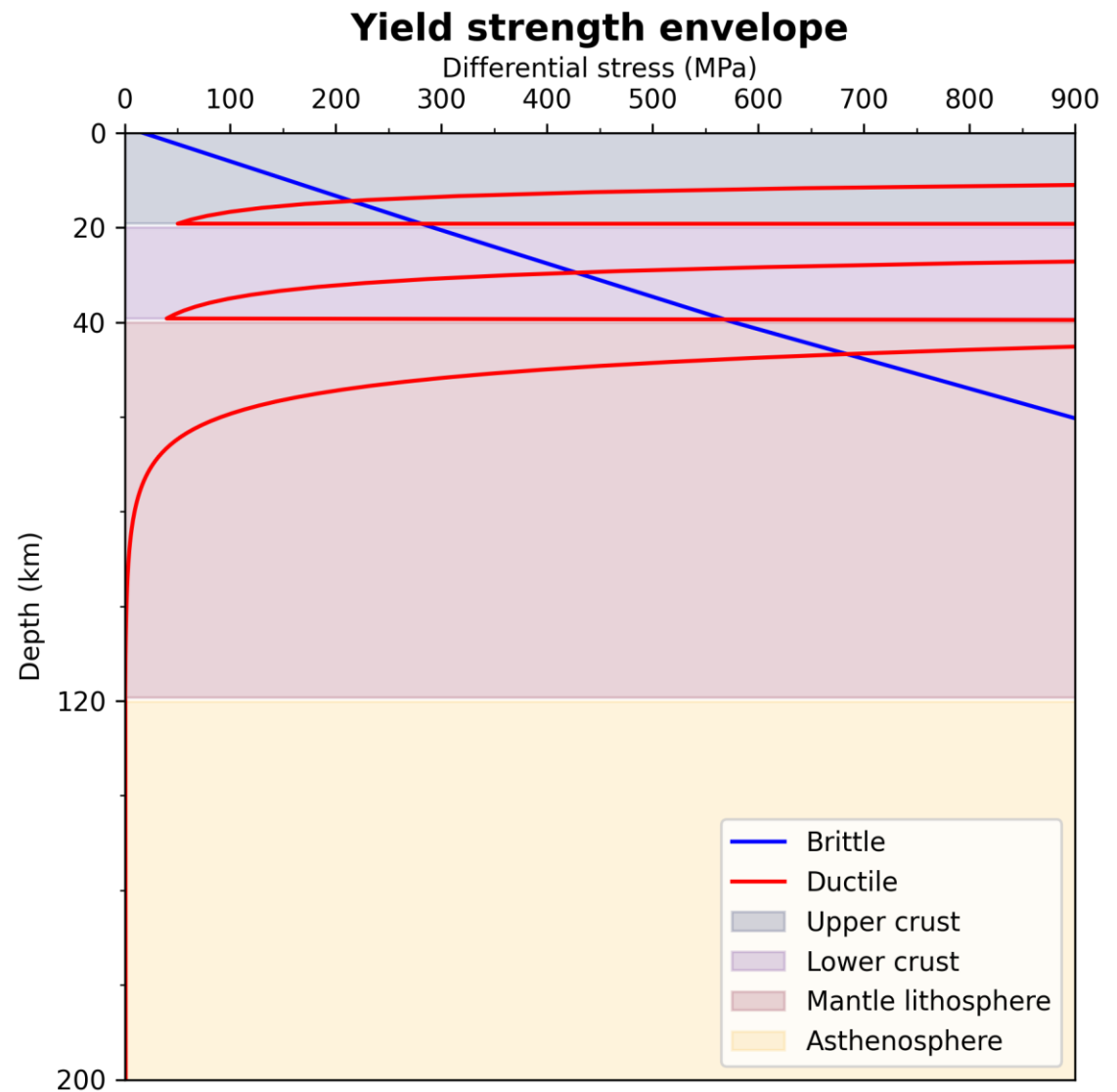
Rheology and flow laws

- Rheology describes the deformation of material.
- Most rocks are **brittle** at room temperature and atmosphere.
- However, they transition to a **ductile** state under mantle-like pressure and temperature.
- The ductile strength of rocks are measured in laboratory experiments (i.e., **flow laws**).
- Here we model both dislocation creep and diffusion creep.



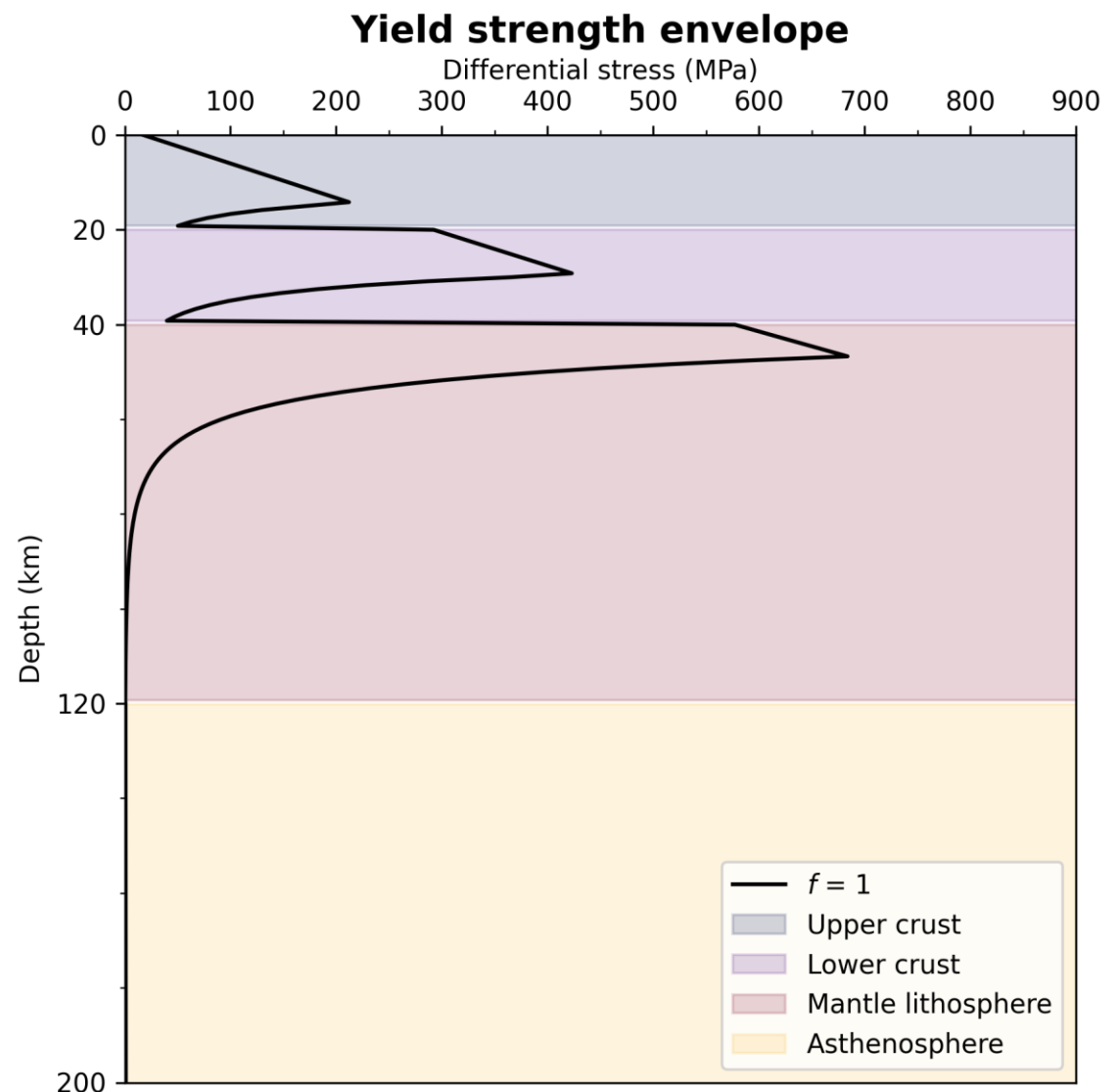
Rheology and flow laws

- ASPECT can simulate both **brittle** and **ductile** deformation.



Rheology and flow laws

- ASPECT can simulate both **brittle** and **ductile** deformation.
- The lithospheric yield strength is determined by the **minimum differential stress** required to deform the rock.

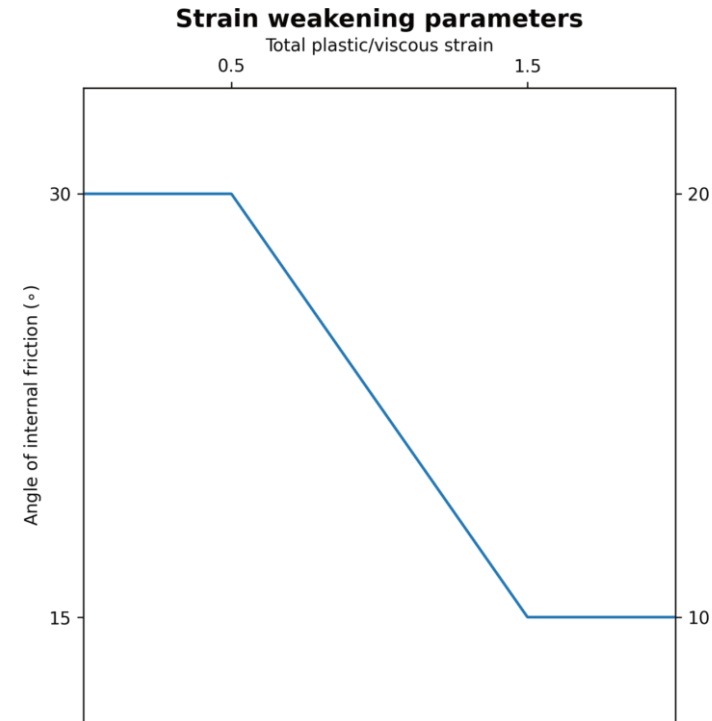


Implementation of structural inheritance

- We use two mechanisms to create structural and rheological heterogeneities.
 - **Strain:** randomly-distributed brittle deformation (to represent varying orogenic deformation)
 - **Rheology:** lower rock strength through viscosity (to represent subduction-related deformation)

$$\sigma'_y = C \cos \phi + P \sin \phi$$

Given sufficient plastic strain, weaken cohesion C and angle of internal friction ϕ



$$\eta = \frac{1}{2} A^{-\frac{1}{n}} d^{\frac{m}{n}} \dot{\varepsilon}_{ii}^{\frac{1-n}{n}} \exp\left(\frac{Q^* + PV^*}{nRT}\right)$$

Scale effective viscosity by modifying material constant A

